© 2020. Published by The Company of Biologists Ltd | Journal of Experimental Biology (2020) 223, jeb221424. doi:10.1242/jeb.221424

RESEARCH ARTICLE

Carbonic anhydrases are influenced by the size and symbiont identity of the aggregating sea anemone *Anthopleura elegantissima*

Jack Cushman Koch[1,*], E. Alan Verde[2] and Virginia M. Weis[1]

ABSTRACT

Carbonic anhydrases (CA; EC 4.2.1.1) play a vital role in dissolved inorganic carbon (DIC) transport to photosynthetic microalgae residing in symbiotic cnidarians. The temperate sea anemone *Anthopleura elegantissima* can occur in three symbiotic states: hosting *Breviolum muscatinei* (brown), hosting *Elliptochloris marina* (green) or without algal symbionts (aposymbiotic). This provides a basis for *A. elegantissima* to be a model for detailed studies of the role of CA in DIC transport. This study investigated the effects of symbiosis, body size and light on CA activity and expression, and suggests that *A. elegantissima* has a heterotrophy-dominated trophic strategy. We identified putative *A. elegantissima* CA genes and performed phylogenetic analyses to infer subcellular localization in anemones. We performed experiments on field-collected anemones to compare: (1) CA activity and expression from anemones in different symbiotic states, (2) CA activity in brown anemones as a function of size, and (3) CA activity in anemones of different symbiotic states that were exposed to different light intensities. CA activity in brown anemones was highest, whereas activity in green and aposymbiotic anemones was low. Several CAs had expression patterns that mirrored activity, while another had expression that was inversely correlated with activity, suggesting that symbionts may induce different DIC transport pathways. Finally, CA activity was inversely correlated with anemone size. Our results suggest that the observed CA activity and expression patterns are affected not only by symbiosis, but also by other factors in the host physiology, including trophic strategy as it relates to body size and cellular pH homeostasis.

KEY WORDS: *Breviolum muscatinei*, Sea anemone, *Elliptochloris marina*, Dissolved inorganic carbon transport, Symbiosis, Cnidarian

INTRODUCTION

Many cnidarians engage in symbioses with photosynthetic microalgae. These holobionts form the structural and trophic bases for coral reef ecosystems and are major components of temperate intertidal ecosystems (reviewed in Shick, 1991). The importance of these symbioses to these ecosystems lies in the nutritional exchange between the host and microalgal symbionts (Harland and Davies, 1995; Muscatine, 1990). The temperate symbiotic sea anemone *Anthopleura elegantissima* is a prominent member of the intertidal ecosystem on the west coast of North America. These anemones rely primarily on heterotrophic nutrition but are facultatively symbiotic and occur in three symbiotic states depending on light intensity and temperature: brown, green and aposymbiotic (Saunders and Muller-Parker, 1997). Brown anemones obtain their color from the presence of the dinoflagellate symbiont *Breviolum muscatinei* (formerly *Symbiodinium*, ITS2 type B4; Lajeunesse and Trench, 2000; LaJeunesse et al., 2018) and occur in high light, warmer environments. In contrast, green anemones harbor the chlorophyte *Elliptochloris marina* and are found in low light, cooler habitats (Letsch et al., 2009; Lewis and Muller-Parker, 2004). Aposymbiotic anemones are white, symbiont-free and are found in very low light or in darkness (Secord and Augustine, 2000). Although both species of microalgae provide photosynthate to their host anemone, *B. muscatinei* is more productive than *E. marina*, thus requiring more dissolved inorganic carbon (DIC) for photosynthesis and passing more organic carbon to the host (Verde and McCloskey, 2007).

Carbonic anhydrases (CAs; EC 4.2.1.1) are critical for DIC transport in symbiotic cnidarians (Al-Moghrabi et al., 1996; Furla et al., 2000a,b; Le Goff et al., 2016; Weis, 1991; Weis and Reynolds, 1999; Weis et al., 1989). Microalgal symbionts are housed deep in host tissue within host gastrodermal cells, making the diffusion of DIC and oxygen from the surrounding seawater difficult. This challenge is compounded by symbiont productivity and animal size because as symbiont productivity increases, so does the requirement for DIC, and as animal size increases, surface-area-to-volume (SA:V) ratios decrease, providing relatively less area for diffusion across cell membranes. Consequently, as expected, Weis et al. (1989) demonstrated that SA:V ratio also affects CA activity when compared across symbiotic cnidarian species.

Previous studies have shown that CA activity is higher in cnidarians with symbionts compared with those without (aposymbiotic; Weis, 1991; Weis and Reynolds, 1999; Weis et al., 1989). Weis and Reynolds (1999) measured gene expression of a cytosolic CA in *A. elegantissima* using semi-quantitative PCR and found that brown *A. elegantissima* had higher expression than aposymbiotic anemones, matching the differential enzyme activity. These studies suggest that CA is inducible and depends on the presence of symbiotic algae.

Previous work suggests that *A. elegantissima* acquires most of its daily nutrition via heterotrophy (Bergschneider and Muller-Parker, 2008). This sets the stage for updating our understanding of how CAs, enzymes that function in autotrophy in symbiotic cnidarians, participate in the trophic strategy of a symbiotic organism under changing environmental conditions (Fig. 1). In this study, we investigate CAs in *A. elegantissima* in more detail by identifying CA paralogs and their phylogenetic placement, thereby inferring

[1]Department of Integrative Biology, Oregon State University, Corvallis, OR 97331, USA. [2]Corning School of Ocean Studies, Maine Maritime Academy, Castine, ME 04420, USA.

*Author for correspondence (jack.c.koch@gmail.com)

J.C.K., 0000-0001-5733-4640; V.M.W., 0000-0002-1826-2848

Received 7 January 2020; Accepted 25 May 2020

Journal of Experimental Biology (2020) 223, jeb221424. doi:10.1242/jeb.221424

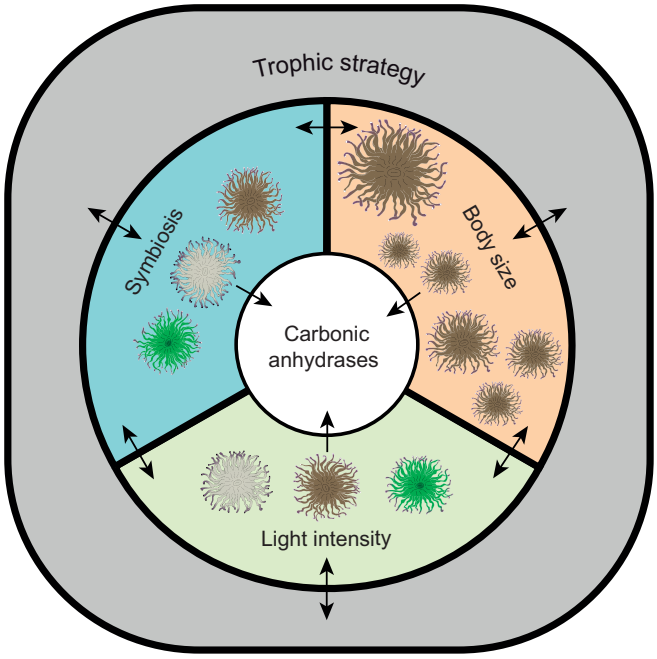

Fig. 1. Diagrammatic representation of the possible role of carbonic anhydrases (CAs) in the interactions between symbiosis, animal size and light that integrate into animal trophic strategy. This study aims to examine CA as a function of these different elements to determine their contribution to trophic strategy.

putative function and location in the cell. We extend the examination of the effect of symbiotic state on CA activity and gene expression of multiple CA paralogs, and provide insight into the effects of animal size and light environment on activity. Consequently, we wanted to answer the following questions: (1) what are the relative concentrations of CA as a function of symbiotic state; and (2) how do a physical factor (light intensity) and a biological factor (anemone size) affect CA activity?

MATERIALS AND METHODS

Experimental manipulations and CA activity measurements of the symbiotic state study were performed at Walla Walla University's Rosario Beach Marine Laboratory (RBML), Anacortes, WA, USA. The light and anemone size experiments on CA activity measurements, and gene expression analyses of the symbiotic state experiment, were conducted at Oregon State University (OSU).

Animal collection and husbandry

The present study used adult *Anthopleura elegantissima* (Brandt 1835) collected at low tide during the summer of 2017 from Sares Head, Fidalgo Island, WA, USA (symbiotic and size experiments), or Lawrence Point, Orcas Island, WA, USA (light experiment). Anemones were removed from rocks using a microspatula, cleaned of all foreign materials (shell and macroalgal bits), immediately flash frozen in liquid nitrogen (symbiotic state and size experiments) or transported back to RBML (light experiment), placed into labeled 118 ml glass jars, and maintained in an outdoor flow-through seawater tank with nylon-stocking-filtered seawater. Flash-frozen anemones were subsequently stored at −80°C until processed. The symbiotic state of anemones in the field was determined by eye during collection and subsequently confirmed in the laboratory by examining tentacle squashes under a microscope. Brown and green anemones were classified as having at least 90% of their respective symbionts, though there were very few anemones that had mixed algal populations.

For the symbiotic state experiment, aposymbiotic anemones (n=10), anemones containing *Elliptochloris marina* (green anemones, n=10) and anemones containing *Breviolum muscatinei* (brown anemones, n=10) were collected from three distinct clones within 3 m of each other. Clones are easily distinguishable by the presence of anemone-free zones that typically separate clonal aggregations and the absence of directed, aggressive acrorhagi deployment (Ayre and Grosberg, 2005; Francis, 1973). When emerged at low tide, *A. elegantissima* retract their tentacles, thereby preventing use of tentacle crown or oral disk diameter as a size measure. Instead, we measured the column crown diameter of each anemone and used it as a proxy for total anemone size. For the size experiment, 20 brown anemones from each size class [small (0–14 mm); medium (15–29 mm); large (>30 mm)] were collected from one clone. For the light experiment, 30 each of aposymbiotic, green and brown anemones were collected.

Sea anemones were collected under Washington Fish and Wildlife permit NESTLER 17-103 to Jim Nestler (Rosario Beach Marine Laboratory, Walla Walla University).

Light environment experiment

An outdoor flow-through seawater tank was modified into three compartments (from inflow to outflow): a cover with several layers of black plastic sheet was added to create a dark environment, neutral density screens were added for a medium light environment, and the last compartment was unmodified for full exposure to the sunlight (high light environment). Light experiment anemones of each symbiotic state (n=10) were randomly divided into the three treatment groups: high (1400 µmol photons m^{-2} s^{-1}), medium (250 µmol photons m^{-2} s^{-1}) or no light. Light intensity in each compartment was measured around 11:00 h daily using the sunlight setting on a QMSW-SS Quantum light meter (Apogee, Logan, UT, USA) and are reported as 28-day averages of single point measurements.

Twenty-four hours after collecting the anemones, they were placed into their respective light treatments and allowed to acclimate for 7 days. Thereafter, five anemones of each symbiotic state and light treatment were flash frozen in liquid nitrogen as a baseline (day 0) for CA activity. Twenty-eight days after the initial sampling, the remaining anemones were flash frozen (day 28) and analyzed for changes in CA activity from the baseline measurements. Every 2 days during acclimation and treatment, anemones were rotated within their treatment areas to eliminate any light differences within compartments. Jars were changed and cleaned every 7 days of the experiment. Over the course of the experiment, the temperature of the seawater ranged from 12.7 to 13.7°C.

Quantification of algae in host anemones

To quantify algae in hosts, a small piece of tissue was cut from each host anemone to include tentacles, oral disc and column tissue. The anemone tissue was homogenized in a known amount of filtered seawater (FSW) in a 2 ml ground-glass homogenizer until no large chunks remained. The resulting homogenate was vortexed for 10 s and algal density was counted in triplicate using a Countess II automated cell counter (Invitrogen, Singapore). To index algal number to host protein, remaining homogenates were centrifuged at 4200 ***g*** in a tabletop centrifuge for 10 min at 4°C to pellet the algae and other cellular debris. The anemone-only protein supernatant was decanted and soluble protein concentration was determined spectrophotometrically using a Bradford protein assay (Bradford, 1976) following the

manufacturer's instructions. Triplicate algal counts were averaged and normalized to soluble anemone protein.

CA activity assay

CA activity was measured as previously described (Weis and Reynolds, 1999) (for full protocol details, see dx.doi.org/10.17504/protocols.io.j4hcqt6). Briefly, on ice in a glass-Teflon homogenizer, one-quarter of each anemone was homogenized in cold enzyme extraction buffer. The resulting homogenate was transferred to a 15 ml tube and centrifuged at 4200 ***g*** for 10 min at 4°C to pellet the algae and cellular debris. The anemone supernatant was decanted and divided into three aliquots destined for native (3 ml), denatured (3 ml) and protein (0.5 to 1 ml) measurements. The denatured sample was boiled for 5 min and placed on ice. In a 6 ml flat-bottom test tube equipped with a tiny stir bar, 1 ml of anemone fraction and 1 ml of cold Buffer A were combined while on ice. When the pH stabilized at 8.2, 1 ml of CO_2-saturated cold deionized water was quickly added. The change in pH of this mixture was recorded using a PH47-SS stainless steel pH probe (Hach, Loveland, CO, USA) attached to an H260GNP pH meter (Hach) writing data to a computer running H-series SmartLogger II (Hach) until the pH stabilized. This was repeated a total of three times for the native and denatured samples. Anemone protein concentration was determined spectrophotometrically using a Bradford protein assay (Bradford, 1976).

Phylogenetic analyses of *A. elegantissima* CAs

Phylogenetic analysis aids in predicting the subcellular location of proteins based on their sequences, domain architecture and groupings with known, well-researched orthologs from other species. Known and predicted AeleCA gene sequences were obtained from Weis and Reynolds (1999) (accession AF14053) and by a gene name search for 'carbonic anhydrase' in the aposymbiotic *A. elegantissima* transcriptome v1.0 database. The working assembly transcriptome for *A. elegantissma* is accessible on Dryad (datadryad.org/resource/doi:10.5061/dryad.3f08f) and raw data are available on NCBI (SRA accession: SRR2300240) (Kitchen et al., 2015a,b). The nucleotide sequences specific for AeleCAs examined in this study are provided in Table S1. Published cnidarian, sponge and human CA protein sequences were obtained from appendix S1 and table S1 in Le Goff et al. (2016).

Open reading frame (ORF) analysis and translation, in all six frames, was performed on all potential AeleCA sequences using Geneious (v10.2.6). Homology of AeleCAs was assessed using Blastp against the NCBI non-redundant database and domain analysis with Pfam. AeleCAs with top hits to other CAs were retained for further domain architecture analyses. Signal peptide, transmembrane domains and subcellular localization motifs were predicted using SignalP (v4.0), TMHMM (v2.0) and TargetP (v1.1), respectively (Table S1). From these analyses, we picked four AeleCA genes representing different predicted subcellular localizations. Protein sequences specific for AeleCAs examined in this study are provided in Table S1.

Protein sequences from Le Goff et al. (2016) and AeleCAs were imported as a single matrix in Mesquite (v3.6) with Zephyr (v3.0) for phylogenetic analyses (http://www.mesquiteproject.org and http://zephyr.mesquiteproject.org). To map the predicted subcellular localization from the Le Goff et al. (2016) phylogenetic tree to ours, we created a taxon matrix with the taxa and predicted CA localization for each. AeleCAs were trimmed of signal peptides and terminal transmembrane domains to only include the section corresponding to the CA catalytic domain as performed in Le Goff et al. (2016). Sequences were aligned using Muscle (v3.8.31) and both model selection and tree inferences were performed using IQTREE ModelFinder and IQTREE nonparametric bootstrap approximation, respectively (Edgar, 2004; Kalyaanamoorthy et al., 2017). The Mesquite and IQTREE files are available at https://github.com/jackckoch/aele.ca.

Preliminary tree inferences suggested that there were several potential rogue taxa in our analysis. Rogue taxa can create instability and generate poor support in phylogenetic analyses, which can obscure and reduce support for relationships among more stable taxa. To identify rogue taxa in our dataset, we used RogueNaRok with an IQTREE nonparametric bootstrap approximation with 100 replicates (Aberer et al., 2013; Nguyen et al., 2015). RogueNaRok identified several potential rogue taxa with one being the most outstanding: *Hydra magnapapillata CA13*. Removal of this taxon improved the relative bipartition information criterion (RBIC) of our tree from 0.502 to 0.529. The RBIC is the sum of all support values divided by the maximum possible support in a fully bifurcating tree, thus a higher RBIC value indicates a larger percentage of the total support possible (Aberer et al., 2013). In our preliminary tree iterations, *H. magnapapillata* CA13 jumped around in the tree, often appearing as the longest branch in the tree; therefore, based on the rogue taxa analysis, this taxon was removed from future tree iterations. Following rogue taxa removal, we re-ran RogueNaRok to check for other potential rogue taxa, but found none that were as outstanding or concerning as *H. magnapapillata CA13*.

According to IQTREE ModelFinder, the best model was WAG+F+R6 according to the Bayesian information criterion (BIC; −Lnl=42,453.063) and WAG+F+R7 according to Akaike's information criterion (AIC; −Lnl=42,450.721), which are both similar to the model used in Le Goff et al. (2016). These models utilize general amino acid exchange rate matrices (WAG; Whelan and Goldman, 2001) that have empirical amino acid frequencies from the data (+F), and a FreeRate model that generalizes the discrete gamma model by relaxing the assumptions of the gamma-distributed rates (+R; Soubrier et al., 2012; Yang, 1995) by the number of categories specified after the model modifier (e.g. +R6 or +R7). AIC and BIC are sets of criteria for model selection. In our analysis, tree building used the stricter, BIC best model and we used IQTREE to create a maximum likelihood tree and evaluated 1000 nonparametric bootstrap approximation replicates to assess branch support (Fig. 2) (Nguyen et al., 2015).

RNA extraction and cDNA synthesis

Total RNA was extracted from anemones collected for the symbiotic state comparison (n=5 per symbiotic state) using a hybrid extraction protocol with TRIzol Reagent (Life Technologies, Eugene, OR, USA) and an RNeasy Mini kit (Qiagen, Valencia, CA, USA) as described by Poole et al. (2016) and stored at −80°C. We performed a cleanup step on all samples following the protocol as described in Poole et al. (2016). Both RNA quality and quantity were assessed using a NanoDrop ND-1000 (NanoDrop, Wilmington, DE, USA) and a Qubit 3.0 fluorometer (Invitrogen, Carlsbad, CA, USA), respectively. The cDNA synthesis was performed with the Protoscript II first strand synthesis system (New England Biolabs, Ipswich, MA, USA) using 150 ng of RNA and the Oligo(dT) primer.

Quantitative PCR (qPCR) experiments

Prior to performing qPCR on the AeleCA genes, reference genes that had stable expression across symbiotic states were determined. We identified several common reference genes used in qPCR experiments with cnidarians [*DNA-directed RNA polymerase*,

Journal of Experimental Biology (2020) 223, jeb221424. doi:10.1242/jeb.221424

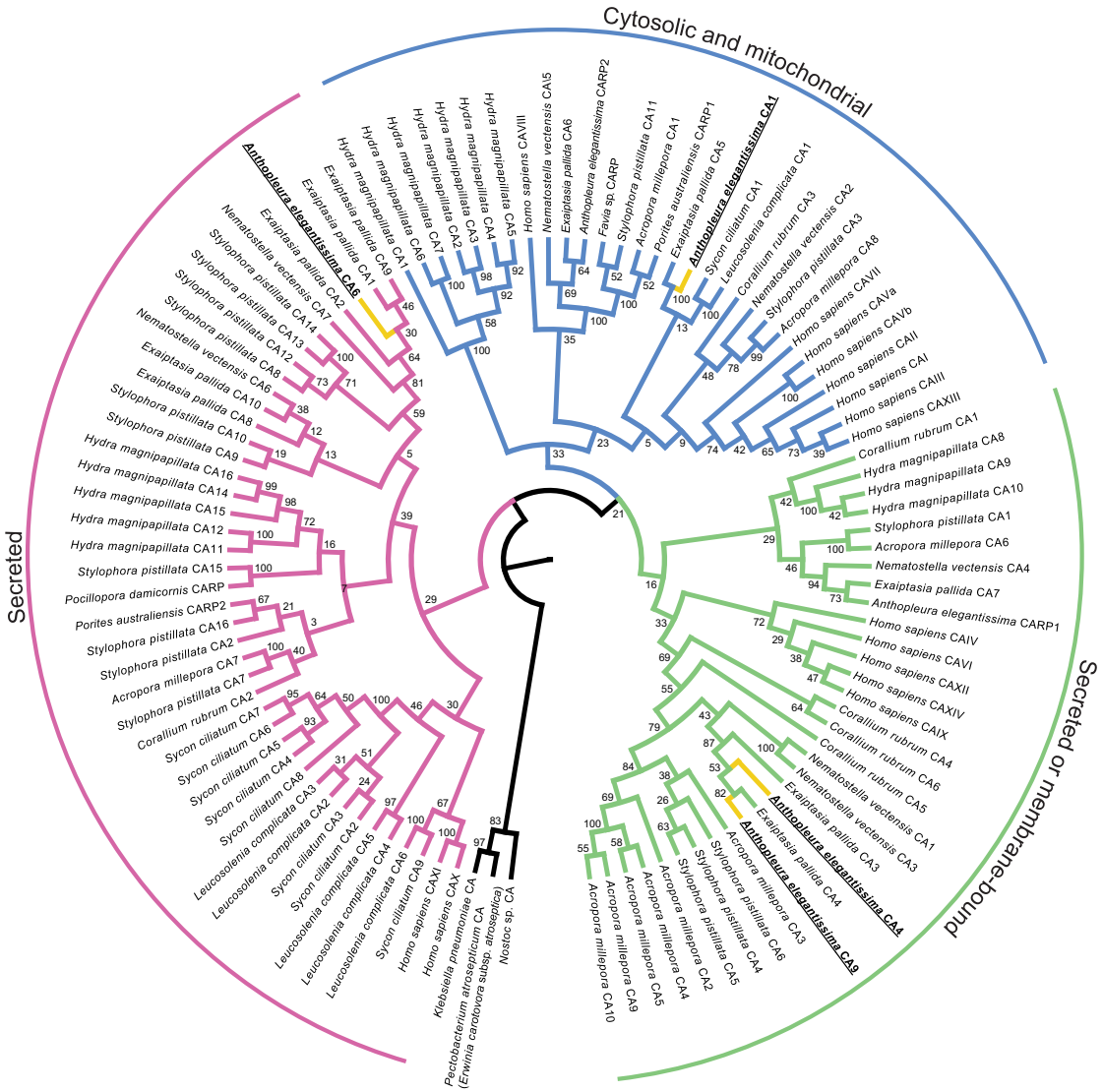

Fig. 2. Maximum likelihood phylogenetic relationships of 104 cnidarian alpha-CA protein sequences adapted from Le Goff et al. (2016). Sequences were aligned with Muscle and the tree was constructed using IQTREE. The presented topology was created using the maximum likelihood method with 1000 non-parametric bootstraps to calculate support values at each node. The bacterial CA sequences from *Pectobacterium atrosepticum* (*Erwinia carotovora* subsp. *atroseptica*), *Klebsiella pneumonia* and *Nostoc* sp. were used as outgroup as in Le Goff et al. (2016). Pink, putative secreted CAs; blue, putative cytosolic CAs; green, putative secreted or membrane-bound CAs; black, outgroup CAs; yellow, *A. elegantissima* CAs examined in this study.

60S ribosomal protein L11, *glyceraldehyde 3-phosphate dehydrogenase* (*G3PD*), *40S ribosomal protein S7*, *and nicotinamide adenine dinucleotide* (*NADH*) *dehydrogenase*; Kenkel et al., 2011; Kitchen et al., 2015b; Leggat et al., 2011; Lehnert et al., 2014; Poole et al., 2016; Radonić et al., 2004; Seneca et al., 2010] and evaluated their expression levels from *A. elegantissima* symbiotic state RNA-seq data (J. C. Koch, personal observation). Of the genes identified, *NADH dehydrogenase* and *G3PD* had the most stable expression across the three anemone symbiotic states.

Specific primers for each AeleCA were designed using Primer3 in Geneious (v10.2.6) to produce 149 bp amplicons (Table S2). Primer efficiencies and optimal template concentration were determined using standard curve analysis with a two-fold dilution series of cDNA from a brown anemone sample and were between 87 and 100% (https://github.com/jackckoch/aele.ca). For each biological replicate, qPCR was performed in triplicate using the Power SYBR® Green PCR Master Mix (Applied Biosystems, Waltham, MA, USA) with premixed ROX in a Mastercycler Realplex4 ep Gradient S (Eppendorf, Germany) under the standard settings, using the following run protocol with the addition of a melt curve: 95°C for 10 min, followed by 40 cycles of 95°C for 15 s, 59°C for 45 s, and 72°C for 15 s. We followed the manufacturer's instructions with the following modification: the total reaction volume was 15 µl, which included 0.45 µl of each forward and reverse primer at 10 µmol, 2 µl of the appropriate cDNA template (total concentration per reaction of 15 ng μl^{-1}), 7.5 µl of Power SYBR Green PCR Master Mix, and 4.6 µl of nuclease-free water. Plates included no-template, no-reverse transcriptase and no-primer controls, and at least one interplate calibrator (IPC).

Data analysis

Data were analyzed in RStudio (v1.1.463) (https://www.rstudio.com/) with R (v3.4.2) (https://www.R-project.org/) and figures were generated with the ggplot2 (v2.2.1) package (Wickham, 2009). R code is available at https://github.com/jackckoch/aele.ca.

Journal of Experimental Biology (2020) 223, jeb221424. doi:10.1242/jeb.221424

For CA activity, time (in seconds) was plotted against the pH of each reaction and the slope between each time point was calculated. The most rapid change in pH from each measurement was averaged with the other replicates. To calculate CA activity, the average slope of the denatured reactions was subtracted from the native reactions and converted to change in pH per minute to be comparable with other CA studies. This CA value was standardized to soluble anemone protein, measured in µg and converted to mg for CA activity calculations, as per the following equation (Weis, 1991):

$$\text{CA activity} = \frac{(\text{pH native animal homogenate} - \text{pH denatured animal homogenate min}^{-1})}{\text{soluble animal protein}}. \quad (1)$$

Normality of distribution was tested with the Shapiro–Wilk test ($P<0.05$) and by visually assessing the distribution of the residuals in the quantile–quantile plots. Data were not normally distributed; however, ANOVAs are robust against normality violations so we ran both parametric and non-parametric analyses. Homogeneity of variance was tested with the Levene's test ($P>0.05$). Differences in CA activity between symbiotic states were tested using a Kruskal–Wallis test ($P<0.05$) followed by a Benjamini–Hochberg corrected *post hoc* Dunn's test (non-parametric) and a two-way ANOVA ($P<0.05$) followed by a *post hoc* Tukey's honest significant difference (HSD) test (parametric). Both tests provided the same results. Differences in CA activity between light environment start and end values were tested using a Student's or Welch's *t*-test ($P<0.05$) where appropriate. Linear models were used to determine which independent variables (e.g. diameter, algal density) best predicted a dependent variable (CA activity).

For CA gene expression, all plates had their baselines and thresholds set to 3–15 and 800, respectively. The crossing threshold (C_t) values from the IPCs across all plates were averaged and necessary corrections for each plate were calculated from that average. Corrected C_t values for qPCR replicates were averaged and imported into RStudio for analysis using the Markov chain Monte Carlo (MCMC) qPCR package (Matz et al., 2013), which converts the C_t values to transcript counts, allowing the analysis of relative gene expression instead of absolute expression. The counts were grouped by gene and symbiotic state and plotted to evaluate the abundance of each gene. We used 39 as the C_t value that represents a single transcript and although this number was not verified on the qPCR machine, we treated all samples the same, lending validity to our analysis of relative gene expression. Aposymbiotic anemones were set as the control group in the experiment. First, we fit a naïve model without reference genes. The summary plot from this model suggested that *NADH dehydrogenase* and *G3PD* both had some variability in expression amongst our treatment groups that needed to be accounted for in our informed model. We fit an informed model (which included normalization to the reference genes) and took into account variation in the stability of reference genes (m.fix=1.5). Differences in the resulting relative quantities on the $\log_2$ scale were tested using Student's *t*-tests ($P<0.05$). Although the model took into account the control group (aposymbiotic anemones) variance, we estimated and visualized the aposymbiotic group variance by setting one of the experimental groups (brown or green anemones) as the control and rerunning our model. When green anemones were set as the control, the credible intervals for the aposymbiotic anemones were larger than when brown anemones were set as the control. For this reason, we modeled green anemones as the control in order to illustrate the credible intervals for the aposymbiotic anemones.

RESULTS

Anthopleura elegantissima CAs group with other metazoan CAs according to putative function and location

We initially identified many potential AeleCAs (https://github.com/jackckoch/aele.ca), but selected four CA paralogs with different putative subcellular locations – secreted, secreted or membrane-bound, membrane-bound, and cytosolic – based on previous research, prediction programs and by adding our AeleCAs to a cnidarian CA phylogeny from Le Goff et al. (2016) (see Materials and Methods, Fig. 2). We named these genes by human CA convention: cytosolic, *AeleCA1*; secreted, *AeleCA6*; membrane-bound, *AeleCA4*; secreted or membrane bound, *AeleCA9*. The resulting phylogenetic tree shows that CAs form distinct clusters based on putative subcellular localization, albeit with weaker support than other published trees (Fig. 2). Most sequences grouped into phylum-specific clusters with AeleCAs always grouping with symbiotic sea anemone *Exaiptasia pallida* CAs within cnidarian clades.

CA activity as a function of symbiotic state

Aposymbiotic and green anemone CA had similar average activities of 0.28±0.09 and 0.38±0.13 $-\Delta$pH min^{-1} mg^{-1} soluble animal protein, respectively ($n=10$), whereas brown anemones had significantly higher average activity of 0.79±0.11 $-\Delta$pH min^{-1} mg^{-1} soluble animal protein (ANOVA, $F=65.65$, $P<0.001$; and Kruskal–Wallis test, $\chi^2=20.612$, $P<0.001$; $n=10$; Fig. 3).

CA gene expression as a function of symbiotic state

For cytosolic *AeleCA1*, there were no significant differences in expression between the three anemone types (Student's *t*-tests: brown–green $P_{MCMC}=0.30$, brown–aposymbiotic $P_{MCMC}=0.81$, green–aposymbiotic $P_{MCMC}=0.43$; Fig. 4A). For putative membrane-bound *AeleCA4*, brown and green anemones had 0.724 and −0.072 mean relative expression, respectively. Brown anemone expression was significantly higher than green anemone expression, but neither were statistically different from that of aposymbiotic anemones (Student's *t*-tests: brown–green $P_{MCMC}<0.05$, brown–aposymbiotic $P_{MCMC}=0.06$, green–aposymbiotic $P_{MCMC}=0.80$; Fig. 4A). For putative secreted *AeleCA6*, brown and green anemones had 1.113 and 0.256 mean relative expression, respectively. Brown anemone expression was significantly higher than aposymbiotic anemone expression (Student's *t*-test: brown–aposymbiotic $P_{MCMC}<0.05$). Brown anemone expression compared with green anemone expression and green anemone expression compared with aposymbiotic anemone expression were not statistically different from each other (Student's *t*-tests: brown–green $P_{MCMC}=0.10$, green–aposymbiotic $P_{MCMC}=0.69$; Fig. 4A). For putative membrane-bound or secreted *AeleCA9*, brown and green anemones had −2.596 and 1.542 mean relative expression, respectively, which were significantly different from each other and from aposymbiotic anemone expression (Student's *t*-tests: $P_{MCMC}<0.001$; Fig. 4A).

We compared the transcript abundance with relative expression, allowing us to illustrate the putative importance of each paralog for each symbiotic state (Fig. 4B). *AeleCA1* had the highest transcript abundance for all three symbiotic states, followed by *AeleCA6* and *AeleCA4* (Fig. 4B and Fig. S2). For all three paralogs, brown anemones had the highest mean abundance. In contrast, *AeleCA9* was most abundant in green anemones, followed by aposymbiotic and brown. *AeleCA9* in brown anemones was the least abundant overall.

CA activity as a function of brown anemone size

CA activity in brown anemone tissue showed a significant inverse correlation with the size of the anemone (linear regression: adjusted $R^2=0.5424$, $P<0.001$; Fig. 5).

Journal of Experimental Biology (2020) 223, jeb221424. doi:10.1242/jeb.221424

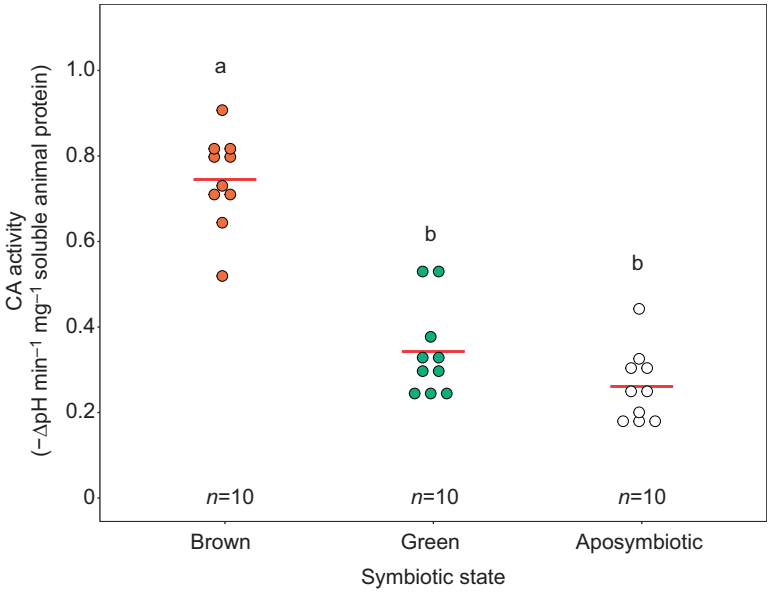

Fig. 3. CA activity from field-collected *A. elegantissima* in different symbiotic states: a 'brown' state (*n*=10) with *Breviolum muscatinei*, a 'green' state (*n*=10) with *Elliptochloris marina* or aposymbiotic (*n*=10) animals lacking symbionts. Each point is the average of triplicate technical replicates, the red line within each group indicates the mean CA activity, and letters indicate statistically significant (α=0.05) difference of the means. Colors represent the three symbiotic states.

CA activity differences with light environment and symbiotic state

With the exception of green anemones exhibiting a significant decrease in average activity after 28 days in the dark compared with day 0 (Student's *t*-test: $P<0.05$; Fig. 6), all other anemone treatment groups showed no significant change in average CA activity after 28 days in their respective light environments with all data points present (Student's *t*-test: $P>0.05$; Fig. 6). However, the day 28 anemones in the green high light and brown darkness groups each had an outlier present as indicated in Fig. 6. After removing the outlier from the day 28 green anemone high light group, there was no significant difference compared with day 0. In contrast, after removing the outlier from the day 28 brown anemone darkness group, there was a significant difference compared with day 0 (Welch's *t*-test: $P<0.001$; Fig. 6).

CA activity as a function of algal density

Regardless of symbiotic state, there were no significant correlations between algal density and CA activity (Figs S1–S3).

DISCUSSION

Green *A. elegantissima* are essentially aposymbiotic anemones in the context of CA activity

Green anemone CA activity was surprisingly lower than expected given that these anemones have a photosymbiont that requires CO_2. The low CA activity in green anemones (not different than aposymbiotic animals; Fig. 3) suggests that green algae DIC demand is met or exceeded by host respiration and diffusion from seawater. Bergschneider and Muller-Parker (2008) came to a similar conclusion from their work examining stable isotope signatures of different *A. elegantissima* symbiotic states. Other research has shown that photosynthetic rates in *E. marina* are much lower than in *B. muscatinei* (Verde and McCloskey, 2002), further supporting the low CA activity measured in our study. Decreased demand for DIC in green anemones could also be explained by differences in the carbon fixing enzyme ribulose-1,5-bisphosphate carboxylase/oxygenase (RubisCO) between the two algal species. Dinoflagellates contain RubisCO form II whereas green algae have form I (Morse et al., 1995; Tabita et al., 2008); form I is more efficient, with a higher affinity for CO_2. Therefore, *E. marina* may be able to acquire enough CO_2 to satisfy DIC needs through diffusion alone whereas *B. muscatinei* cannot, thus inducing the host to increase CA synthesis and activity as a compensatory mechanism.

CA activity does not match expression across all CA paralogs in *A. elegantissima*

Our observed high CA activity in brown versus aposymbiotic anemones recapitulates earlier experiments on *A. elegantissima* (Weis and Reynolds, 1999); however, expression patterns between the two studies are not congruent. We showed no difference in *AeleCA1* (cytosolic) gene expression between symbiotic states (Fig. 4A), a pattern opposite of that observed by Weis and Reynolds (1999). *AeleCA4* (putative secreted or membrane-bound) and *AeleCA6* (putative secreted) expression patterns matched the overall CA activity patterns. *AeleCA1* and likely *AeleCA6* are internal CAs (cytosolic and not attached to a cell membrane) (Weis and Reynolds, 1999). It is more difficult to determine whether *AeleCA4* and *AeleCA9* are internal or external because they could localize to internal or external membranes (Fig. 7). Further research to definitively localize *A. elegantissima* CAs will be critical to fully interpret the results of our study in the context of the symbiotic relationship.

The CA activity assay does not discriminate between different CA paralogs and it is likely that not all CA protein types were captured in animal homogenizations. Extracellular CA might be lost and any membrane-bound CAs might be pelleted with membranes and therefore not end up being measured in the assay. Furthermore, we made no measurement of CA protein turnover, so expression quantity and protein quantity are not necessarily congruent.

The observed pattern in *AeleCA9* (putative secreted or membrane-bound) of high abundance and expression in green anemones and low in brown compared with aposymbiotic anemones suggests that this CA is not an important player in brown anemones (Fig. 4B and Fig. S2). The high expression and abundance of *AeleCA9* in green anemones could indicate that the presence of *E. marina* induces different DIC pathways than does the presence of *B. muscatinei* (Fig. 7). These pathway changes could include differential expression and use of CAs, H^+-ATPases, HCO_3^- transporters and paracellular pathways (Allemand et al., 1998;

Journal of Experimental Biology (2020) 223, jeb221424. doi:10.1242/jeb.221424

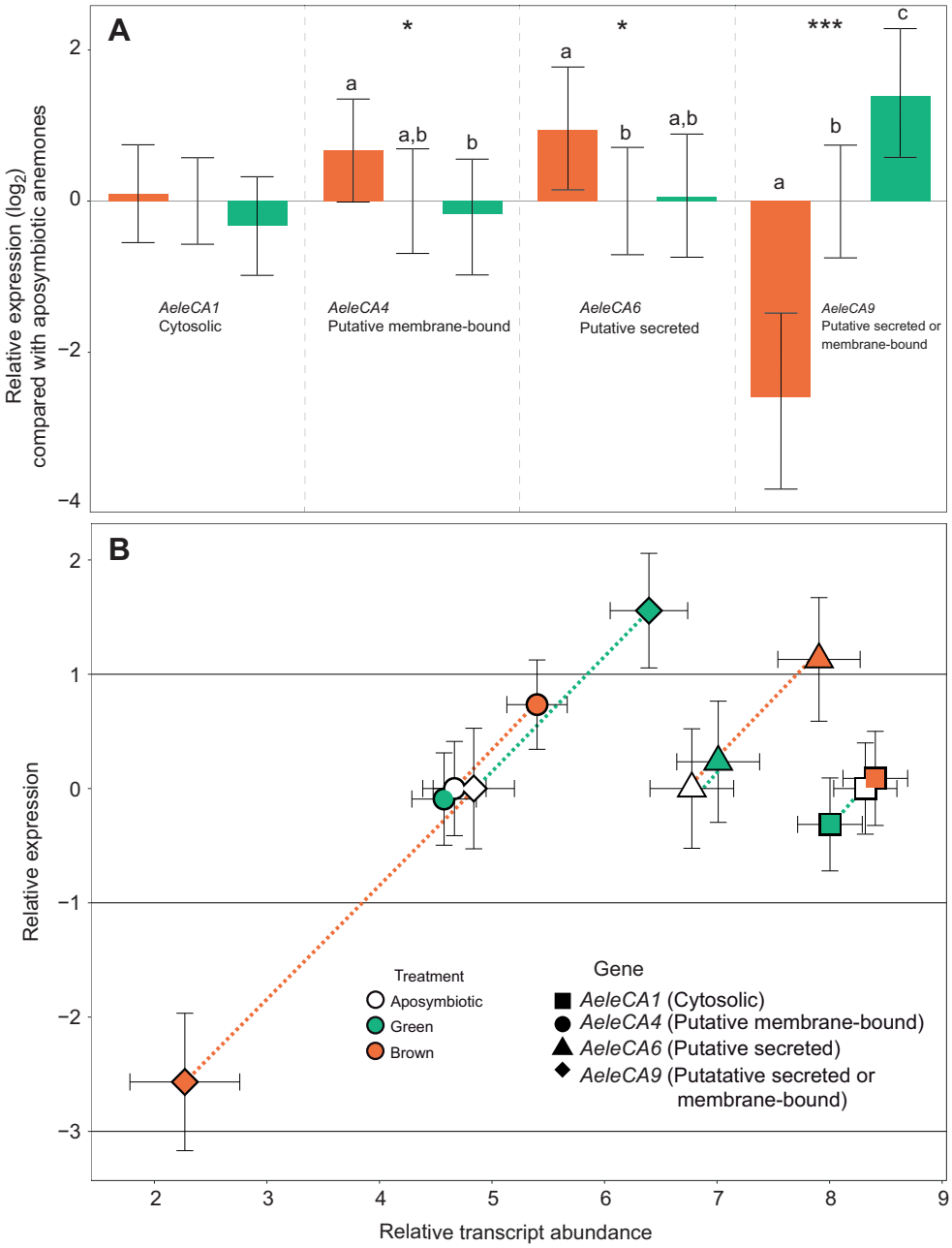

Fig. 4. Gene expression of four different CA paralogs in *A. elegantissima*. (A) Relative gene expression (log_2) and (B) relative transcript abundance (log_2) compared with relative gene expression (log_2) of four CA paralogs from *A. elegantissima* in different symbiotic states (n=5) normalized to *NADH* and *G3PD* and relative to expression in the aposymbiotic state. (A) Asterisks are levels of statistical significance (*$P \leq 0.05$, ***$P<0.001$) and letters indicate statistically significant difference of the means based on *t*-test with $\alpha=0.05$. (B) Dashed lines are drawn between the aposymbiotic anemones and the brown or green anemones, as indicated by the color of the dashed line, for each gene. Error bars in A and B represent the 95% Bayesian credible intervals. Colors represent the three symbiotic states.

Barott et al., 2015a,b; Furla et al., 2000a; Oakley et al., 2016; Tresguerres et al., 2017).

The patterns displayed by *AeleCA9* have parallels to the results of Tansik et al. (2015, 2017), who used membrane inlet mass spectrometry (MIMS) to measure CA activity in corals and their symbionts by calculating the ^{18}O rate of exchange and following labeled $^{13}CO_2$ species. They parsed internal (cytosolic) and external (facing outwards or secreted outside of the cell membrane) CA activity measurements by blocking external CAs with the membrane-impermeable CA inhibitor acetazolamide. Tansik et al. (2015, 2017) showed that algal symbionts of the corals *Orbicella faveolata*, *Porites astreoides* and *Siderastrea radians* had internal CA activity values that correlated with their maximal photosynthesis rate rank: *P. astreoides*, *S. radians* and *O. faveolata* (highest to lowest average rate) (Tansik et al., 2017). *Porites astreoides* and *S. radians* had the lowest external CA activity, yet their symbionts were the most productive. These two corals mirror the pattern of putative external *AeleCA9* expression and symbiont productivity in brown *A. elegantissima* in that *B. muscatinei* have higher productivity compared with *E. marina* (Tansik et al., 2017; Verde and McCloskey, 1996). This suggests that the Symbiodiniaceae species of all three corals and *A. elegantissima* are capable of maximal photosynthesis with limited DIC (Tansik et al., 2017) and could indicate a host-controlled carbon environment as proposed by Davy et al. (2012) and Weis (1993) to limit symbiont growth, reproduction and photosynthetic rates in favor of passing photosynthate to their cnidarian hosts.

In contrast, *O. faveolata* had the highest external CA activity, providing ample DIC for its low-productivity symbionts. This pattern mirrors what we observed in green anemones, which had high *AeleCA9* gene expression (Fig. 4A) and low photosynthetic rates compared with their brown counterparts. We propose that

Journal of Experimental Biology (2020) 223, jeb221424. doi:10.1242/jeb.221424

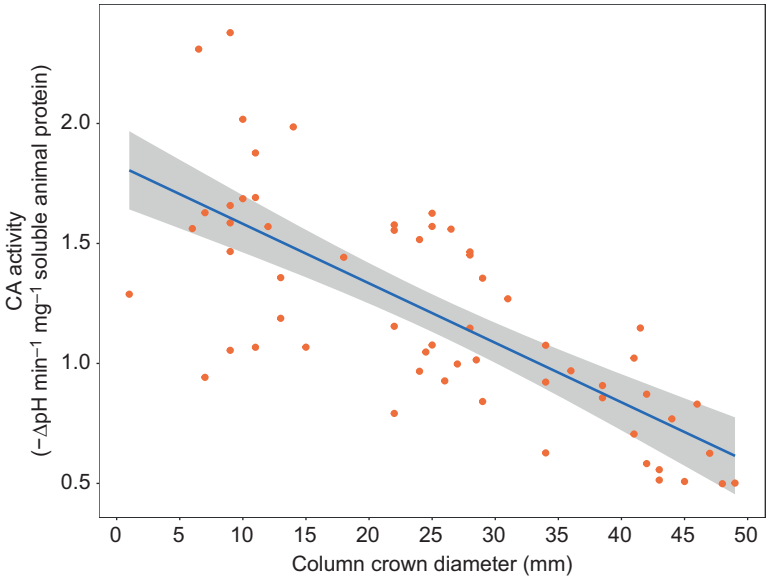

Fig. 5. CA activity from field-collected brown *A. elegantissima* as a function of column crown diameter. Each point is the average of triplicate technical replicates (see Materials and Methods). A linear model was fitted to the data, indicated by the blue line (y=−0.024790x+1.829638; adjusted R^2=0.5424; F>70.92; P<0.001), with standard error of the model represented by the extent of the gray region around the line.

green anemones have adequate external CA activity from *AeleCA9* that, in turn, provides a carbon-sufficient environment for their symbionts (Fig. 7), but that *AeleCA9* activity was not captured by our activity assay because AeleCA9 proteins may be pelleted with the host membranes (see Materials and Methods, and above).

The congruence between photosynthetic rate and host DIC supply in Tansik et al. (2017) suggests that the corals in their study have adapted CAs to support their algal symbionts. In contrast, our work with *A. elegantissima* suggests that CAs are influenced by the phenotype of the symbiosis and that CAs could change if symbiont identity changes (see Bates, 2000 for symbiont switching in *Anthopleura*). Future studies using a single clone in different symbiotic states to examine the subcellular location for the different CA paralogs and tissue-specific CA activity and expression could help reveal their roles in the symbiosis.

Size matters for CA activity of brown *A. elegantissima*, but not as predicted

Anemone size had a strong, inverse effect on CA activity in brown *A. elegantissima* of differing column crown diameters (Fig. 5). Our findings contrast previous work in symbiotic cnidarians that found cnidarians with low surface-area-to-volume ratios to have high CA activity compared with cnidarians with higher surface-area-to-volume ratios (Weis et al., 1989). Of note, size-based CA activity in our study is within or above the range of activity measured for brown anemones in the symbiotic state experiment.

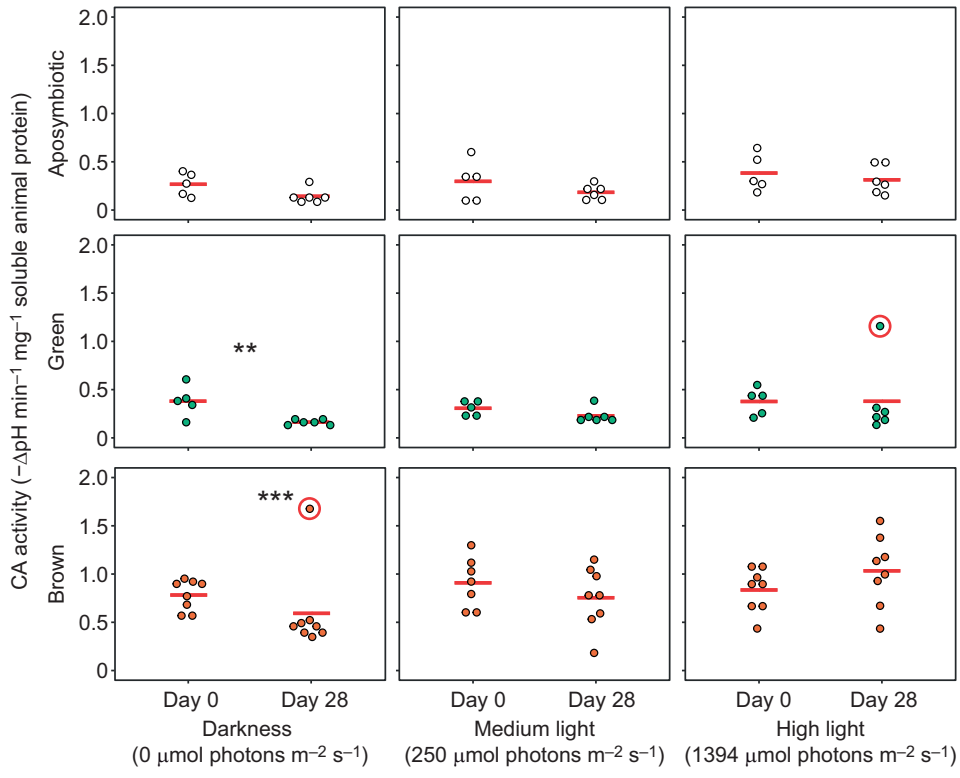

Fig. 6. CA activity of *A. elegantissima* of each symbiotic state placed into different light environments (*n*=5–8). Graph rows are grouped by symbiotic state of the sea anemones and columns are grouped by light treatment. Each point is the average of triplicate technical replicates and the red line within each group indicates the mean CA activity. *P*-value for pairwise comparison of start and end groups with statistically significant (α=0.05) difference of the means are indicated where appropriate. Outliers are circled (red) and have an asterisk (red) next to them where removal of the outlier resulted in a statistically significant *P*-value for pairwise comparison of start and end group difference of the means (α=0.05). Numbers in parentheses indicate the 28-day average light intensity per treatment measured daily at approximately 11:00 h.

Journal of Experimental Biology (2020) 223, jeb221424. doi:10.1242/jeb.221424

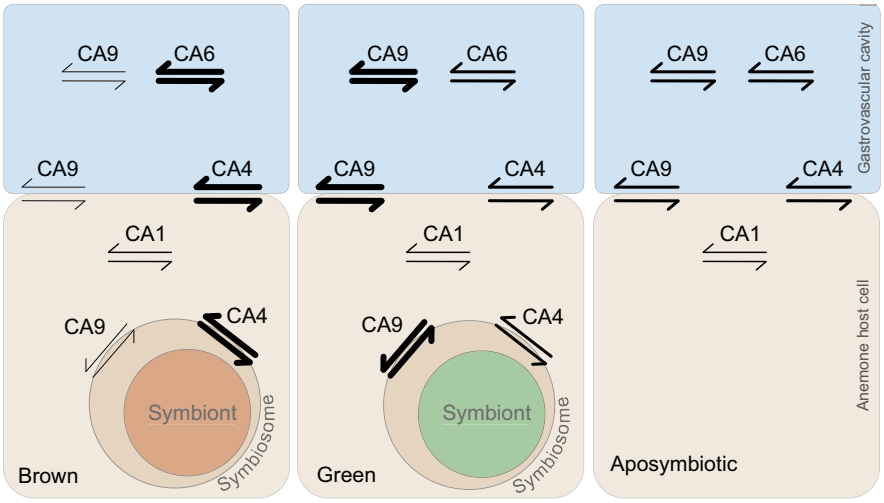

AeleCA1 (Cytosolic)
AeleCA4 (Putative membrane-bound)
AeleCA6 (Putative secreted)
AeleCA9 (Putatative secreted or membrane-bound)

Fig. 7. Brown, green and aposymbiotic anemone gastrodermal cell model of CA paralog putative localization and relative expression based on phylogenetic tree and gene expression studies, respectively. Thickness of arrows represents relative gene expression. Outer circle around symbiont is the host-derived symbiosome membrane complex (symbiosome). Note that our activity and expression measurements are from whole-animal homogenate, not a single tissue layer or type.

The inverse correlation between column crown diameter and CA activity might be explained by a combination of trophic strategy and buffering potential that would determine how much CA is needed to satisfy algal DIC demands and maintain cellular homeostasis. Using stable isotope analysis, previous research has shown that *A. elegantissima* generally relies more heavily on heterotrophy to satisfy daily nutritional needs rather than autotrophic carbon supplied by their algal symbionts (Bergschneider and Muller-Parker, 2008). Larger individuals could therefore be acquiring a greater percentage of their daily carbon and nitrogen nutrition by heterotrophic feeding while smaller individuals could be relying more heavily on symbiont autotrophy. This idea is supported by previous research showing that larger individuals have greater tentacle and prey capture surface area (Sebens, 1981; Zamer, 1986) and research using stable isotope analysis showing that larger individuals from the genus *Anthopleura* rely more heavily on heterotrophy to satisfy daily nutritional needs compared with smaller anemones (Bedgood and Bracken, 2020). Thus, there may be a greater demand for DIC in smaller anemones from their algal symbionts, thereby inducing higher CA activity. Furthermore, algae symbiotic with smaller *A. elegantissima* are fixing more carbon per day relative to large *A. elegantissima* (E. A. Verde, personal observation), also supporting the increase in CA activity that we measured in smaller individuals.

Smaller body sizes favor increased diffusion of gases (e.g. CO_2 and O_2) related to an increased surface-area-to-volume ratio (Brown and Sibly, 2006; Pörtner, 2002), and this may reduce the buffering capacity of small organisms to environmental change. In addition to its role in symbiosis, CA also plays a role in intracellular pH homeostasis (Tashian, 1989). Small anemones may be increasing CA activity to increase their capacity to maintain pH homeostasis. Consequently, the high CA activity observed in small anemones might be induced by a combination of trophic and buffering capacity differences with anemone size.

Light has a modest influence on CA activity in *A. elegantissima*

Given that algal productivity is dependent on light level (Dimond et al., 2013; Verde and McCloskey, 2002, 2007), we predicted that light intensity would affect carbon-concentrating mechanisms for DIC delivery to algae in *A. elegantissima*, as measured by CA activity. We hypothesized that activity in brown and green anemones in the dark, and green anemones in high light would decrease the most compared with brown and green anemones in high and medium light, respectively, because photosynthesis would cease or be affected by photoinhibition, thereby reducing the need for CA-supplied DIC. Our results for the two symbiotic groups placed in darkness supports this hypothesis and conclusions from research by Dimond et al. (2013) that examined symbiont photophysiology under different light intensities. Green anemones placed in high light for 28 days showed a modest decrease in CA activity after removing an outlier, but the change was not significant. For our control groups (i.e. groups that were kept in their respective light environment) and the other light groups, there were no significant changes in CA activity with light.

There are several possible explanations for this stability in activity in some groups across light levels. Firstly, the anemones could have acclimated to their experimental light environments during the 7-day acclimation period of the experiment (see Materials and Methods). CA half-life and degradation rates were not examined in our study but are known to be variable between different tissue types and different organisms (30–80 h in different mouse tissues: McAvoy et al., 1981; 8 h half-life in *Chlamydomonas*: Toguri et al., 1989). Secondly, the experiment duration could have been too short, although with an experimental exposure to the various light regimes for 28 days, this possibility seems remote for most groups. A possible exception may be for the green anemones in high light that, given more time, might have decreased CA activity even further as the effects of high-light-induced algal photoinhibition reached the anemone. Thirdly, we did not control for animal size in this experiment. Based on our result of differential CA activity with animal size (see Fig. 5), it is possible that size differences masked a light effect. Finally, light simply may not play a large role in CA induction because photosynthetic symbionts are not the primary suppliers of host nutrition. *Anthopleura elegantissima* may instead rely largely on heterotrophic nutrition (Bergschneider and Muller-Parker, 2008; Levine and Muller-Parker, 2012) and might therefore be less responsive to changes in light, especially in the short term. Instead of a change in autotrophy-related nutrition (e.g. a change in CA activity), Hiebert and Bingham (2012) showed a general increase in heterotrophy by brown, green and aposymbiotic

anemones in sunlight compared with in shade, supporting our findings and a general dominance of heterotrophy in *A. elegantissima* regardless of symbiotic state. However, seasonal changes in CA activity are a strong possibility because light regimes, temperature profiles and zooplankton density are lower during the winter than during summer months (Dimond et al., 2013; Verde and McCloskey, 2007).

Conclusions

Our study examined the effects of symbiosis, animal body size and light on CAs in a temperate symbiotic sea anemone and their integration into animal trophic strategy (Fig. 1). We found that not just one, but all three factors contribute to the dominance of heterotrophy in *A. elegantissima*. Our data suggest that, based on the behavior of CAs, symbiosis with autotrophic algae is a source of nutrition for these anemones, more so in brown anemones compared with green and aposymbiotic anemones, but as an accessory to heterotrophy in these organisms.

Acknowledgements

We thank Brian Bingham, Jay Dimond and Nate Schwarck at the Shannon Point Marine Center for their advice and assistance in locating anemones, and Nancy Nestler, Jim Nestler, Chris Lindsey, Flora Gibbs, Katie Pekar and Monica Culler at the Rosario Beach Marine Laboratory for their assistance in collecting anemones. Many thanks to Billie Swalla at Friday Harbor Laboratories for use of a plate reader for protein analyses. Thank you to David Maddison and Antonio Gomez for advice and assistance with our phylogenetic analysis and Mesquite usage, and Doug Warrick and Mike Brawner for their discussions about metabolism and scaling. Thanks to Trevor Tivey, John Parkinson, Katherine Dziedzic and Eli Meyer for their assistance with qPCR and advice on data analysis. Special thanks to Valeri Lapacek, Jason Presnell, Allie Graham, Shumpei Maruyama, Nathan Kirk and two reviewers for their discussions and critical comments, which helped to improve the manuscript.

Competing interests

The authors declare no competing or financial interests.

Author contributions

Conceptualization: J.C.K., E.A.V., V.M.W.; Methodology: J.C.K., E.A.V., V.M.W.; Software: J.C.K.; Validation: J.C.K., E.A.V., V.M.W.; Formal analysis: J.C.K.; Investigation: J.C.K., E.A.V., V.M.W.; Resources: J.C.K., E.A.V., V.M.W.; Data curation: J.C.K.; Writing - original draft: J.C.K.; Writing - review & editing: J.C.K., E.A.V., V.M.W.; Visualization: J.C.K.; Supervision: J.C.K., E.A.V., V.M.W.; Project administration: J.C.K., V.M.W.; Funding acquisition: J.C.K., V.M.W.

Funding

This study was supported by funds from the National Science Foundation Graduate Research Fellowship (J.C.K.), the Northwest Scientific Association (student grant to J.C.K.), and the Oregon State University Department of Integrative Biology (zoology research funds to J.C.K. and departmental funds to V.M.W.).

Data availability

Data are available at https://github.com/jackckoch/aele.ca.

Supplementary information

Supplementary information available online at
https://jeb.biologists.org/lookup/doi/10.1242/jeb.221424.supplemental

References

Aberer, A. J., Krompass, D. and Stamatakis, A. (2013). Pruning rogue taxa improves phylogenetic accuracy: an efficient algorithm and webservice. *Syst. Biol.* **62**, 162-166. doi:10.1093/sysbio/sys078

Al-Moghrabi, S., Goiran, C., Allemand, D., Speziale, N. and Jaubert, J. (1996). Inorganic carbon uptake for photosynthesis by the symbiotic coral–dinoflagellate association II. Mechanisms for bicarbonate uptake. *J. Exp. Mar. Biol. Ecol.* **199**, 227-248. doi:10.1016/0022-0981(95)00202-2

Allemand, D., Furla, P. and Bénazet-Tambutté, S. (1998). Mechanisms of carbon acquisition for endosymbiont photosynthesis in Anthozoa. *Can. J. Bot.* **76**, 925-941. doi:10.1139/cjb-76-6-925

Ayre, D. J. and Grosberg, R. K. (2005). Behind anemone lines: factors affecting division of labour in the social cnidarian *Anthopleura elegantissima*. *Anim. Behav.* **70**, 97-110. doi:10.1016/j.anbehav.2004.08.022

Barott, K. L., Venn, A. A., Perez, S. O., Tambutté, S. and Tresguerres, M. (2015a). Coral host cells acidify symbiotic algal microenvironment to promote photosynthesis. *Proc. Natl. Acad. Sci. USA* **112**, 607-612. doi:10.1073/pnas.1413483112

Barott, K. L., Perez, S. O., Linsmayer, L. B. and Tresguerres, M. (2015b). Differential localization of ion transporters suggests distinct cellular mechanisms for calcification and photosynthesis between two coral species. *Am. J. Physiol. Regul. Integr. Comp. Physiol.* **309**, R235-R246. doi:10.1152/ajpregu.00052.2015

Bates, A. (2000). The intertidal distribution of two algal symbionts hosted by *Anthopleura xanthogrammica* (Brandt 1835). *J. Exp. Mar. Bio. Ecol.* **249**, 249-262. doi:10.1016/S0022-0981(00)00203-3

Bedgood, S. A. and Bracken, M. E. S. (2020). Making it big and losing friends: algal symbiont contributions are shaped by sea anemone life history. *Integr. Comp. Biol.* **60**, e14.

Bergschneider, H. and Muller-Parker, G. (2008). Nutritional role of two algal symbionts in the temperate sea anemone *Anthopleura elegantissima* (Brandt). *Biol. Bull.* **215**, 73-88. doi:10.2307/25470685

Bradford, M. M. (1976). A rapid and sensitive method for the quantitation of microgram quantities of protein utilizing the principle of protein-dye binding. *Anal. Biochem.* **72**, 248-254. doi:10.1016/0003-2697(76)90527-3

Brown, J. H. and Sibly, R. M. (2006). Life-history evolution under a production constraint. *Proc. Natl. Acad. Sci. USA* **103**, 17595-17599. doi:10.1073/pnas.0608522103

Davy, S. K., Allemand, D. and Weis, V. M. (2012). Cell biology of cnidarian–dinoflagellate symbiosis. *Microbiol. Mol. Biol. Rev.* **76**, 229-261. doi:10.1128/MMBR.05014-11

Dimond, J. L., Bingham, B. L., Muller-Parker, G. and Oakley, C. A. (2013). Symbiont physiology and population dynamics before and during symbiont shifts in a flexible algal–cnidarian symbiosis. *J. Phycol.* **49**, 1074-1083. doi:10.1111/jpy.12112

Edgar, R. C. (2004). MUSCLE: multiple sequence alignment with high accuracy and high throughput. *Nucleic Acids Res.* **32**, 1792-1797. doi:10.1093/nar/gkh340

Francis, L. (1973). Clone specific segregation in the sea anemone *Anthopleura elegantissima*. *Biol. Bull.* **144**, 64-72. doi:10.2307/1540147

Furla, P., Allemand, D. and Orsenigo, M.-N. (2000a). Involvement of H^+-ATPase and carbonic anhydrase in inorganic carbon uptake for endosymbiont photosynthesis. *Am. J. Physiol. Regul. Integr. Comp. Physiol.* **278**, R870-R881. doi:10.1152/ajpregu.2000.278.4.R870

Furla, P., Galgani, I., Durand, I. and Allemand, D. (2000b). Sources and mechanisms of inorganic carbon transport for coral calcification and photosynthesis. *J. Exp. Biol.* **203**, 3445-3457.

Harland, A. D. and Davies, P. S. (1995). Symbiont photosynthesis increases both respiration and photosynthesis in the symbiotic sea anemone *Anemonia viridis*. *Mar. Biol.* **123**, 715-722. doi:10.1007/BF00349114

Hiebert, T. C. and Bingham, B. L. (2012). The effects of symbiotic state on heterotrophic feeding in the temperate sea anemone *Anthopleura elegantissima*. *Mar. Biol.* **159**, 939-950. doi:10.1007/s00227-011-1871-8

Kalyaanamoorthy, S., Minh, B. Q., Wong, T. K. F., von Haeseler, A. and Jermiin, L. S. (2017). ModelFinder: fast model selection for accurate phylogenetic estimates. *Nat. Methods* **14**, 587-589. doi:10.1038/nmeth.4285

Kenkel, C. D., Aglyamova, G., Alamaru, A., Bhagooli, R., Capper, R., Cunning, R., deVillers, A., Haslun, J. A., Hédouin, L., Keshavmurthy, S. et al. (2011). Development of gene expression markers of acute heat-light stress in reef-building corals of the genus *Porites*. *PLoS ONE* **6**, e26914. doi:10.1371/journal.pone.0026914

Kitchen, S. A., Crowder, C. M., Poole, A. Z., Weis, V. M. and Meyer, E. (2015a). Data from: de novo assembly and characterization of four anthozoan (phylum Cnidaria) transcriptomes, Dryad, Dataset, https://doi.org/10.5061/dryad.3f08f

Kitchen, S. A., Crowder, C. M., Poole, A. Z., Weis, V. M. and Meyer, E. (2015b). De novo assembly and characterization of four anthozoan (Phylum Cnidaria) transcriptomes. *G3* **5**, 2441-2452. doi:10.1534/g3.115.020164

LaJeunesse, T. C. and Trench, R. K. (2000). Biogeography of two species of *Symbiodinium* (Freudenthal) inhabiting the intertidal sea anemone *Anthopleura elegantissima* (Brandt). *Biol. Bull.* **199**, 126-134. doi:10.2307/1542872

LaJeunesse, T. C., Parkinson, J. E., Gabrielson, P. W., Jeong, H. J., Reimer, J. D., Voolstra, C. R. and Santos, S. R. (2018). Systematic revision of Symbiodiniaceae highlights the antiquity and diversity of coral endosymbionts. *Curr. Biol.* **28**, 2570-2580.e6. doi:10.1016/j.cub.2018.07.008

Le Goff, C., Ganot, P., Zoccola, D., Caminiti-Segonds, N., Allemand, D. and Tambutté, S. (2016). Carbonic anhydrases in cnidarians: novel perspectives from the octocorallian *Corallium rubrum*. *PLoS ONE* **11**, e0160368. doi:10.1371/journal.pone.0160368

Leggat, W., Seneca, F., Wasmund, K., Ukani, L., Yellowlees, D. and Ainsworth, T. D. (2011). Differential responses of the coral host and their algal symbiont to thermal stress. *PLoS ONE* **6**, e26687. doi:10.1371/journal.pone.0026687

Lehnert, E. M., Mouchka, M. E., Burriesci, M. S., Gallo, N. D., Schwarz, J. A. and Pringle, J. R. (2014). Extensive differences in gene expression between symbiotic and aposymbiotic cnidarians. *G3* **4**, 277-295. doi:10.1534/g3.113.009084

Letsch, M. R., Muller-Parker, G., Friedl, T. and Lewis, L. A. (2009). *Elliptochloris marina* sp. nov. (Trebouxiophyceae, Chlorophyta), symbiotic green alga of the temperate pacific sea anemones *Anthopleura xanthogrammica* and *A. elegantissima* (Anthozoa, Cnidaria). *J. Phycol.* **45**, 1127-1135. doi:10.1111/j.1529-8817.2009.00727.x

Levine, M. R. and Muller-Parker, G. (2012). Distribution patterns and nutritional contributions of algal symbionts in the sea anemone *Anthopleura xanthogrammica*. *Mar. Ecol. Prog. Ser.* **453**, 79-94. doi:10.3354/meps09602

Lewis, L. A. and Muller-Parker, G. (2004). Phylogenetic placement of "zoochlorellae" (Chlorophyta), algal symbiont of the temperate sea anemone *Anthopleura elegantissima*. *Biol. Bull.* **207**, 87-92. doi:10.2307/1543583

Matz, M. V., Wright, R. M. and Scott, J. G. (2013). No control genes required: Bayesian analysis of qRT-PCR data. *PLoS ONE* **8**, e71448. doi:10.1371/journal.pone.0071448

McAvoy, J., Kuter, M. and Masters, C. (1981). The turnover characteristics of carbonic anhydrase in mouse tissues. *Int. J. Biochem.* **13**, 457-461. doi:10.1016/0020-711X(81)90118-X

Morse, D., Salois, P., Markovic, P. and Hastings, J. W. (1995). A nuclear-encoded form II RuBisCO in dinoflagellates. *Science* **268**, 1622-1624. doi:10.1126/science.7777861

Muscatine, L. (1990). The role of symbiotic algae in carbon and energy flux in reef corals. In *Ecosystems of the World* (ed. Z. Dubinsky), pp. 75-87. Amsterdam: Elsevier Science.

Nguyen, L.-T., Schmidt, H. A., von Haeseler, A. and Minh, B. Q. (2015). IQ-TREE: a fast and effective stochastic algorithm for estimating maximum-likelihood phylogenies. *Mol. Biol. Evol.* **32**, 268-274. doi:10.1093/molbev/msu300

Oakley, C. A., Ameismeier, M. F., Peng, L., Weis, V. M., Grossman, A. R. and Davy, S. K. (2016). Symbiosis induces widespread changes in the proteome of the model cnidarian *Aiptasia*. *Cell. Microbiol.* **18**, 1009-1023. doi:10.1111/cmi.12564

Poole, A. Z., Kitchen, S. A. and Weis, V. M. (2016). The role of complement in cnidarian-dinoflagellate symbiosis and immune challenge in the sea anemone *Aiptasia pallida*. *Front. Microbiol.* **7**, 519. doi:10.3389/fmicb.2016.00519

Pörtner, H. O. (2002). Environmental and functional limits to muscular exercise and body size in marine invertebrate athletes. *Comp. Biochem. Physiol. A Mol. Integr. Physiol.* **133**, 303-321. doi:10.1016/S1095-6433(02)00162-9

Radonić, A., Thulke, S., Mackay, I. M., Landt, O., Siegert, W. and Nitsche, A. (2004). Guideline to reference gene selection for quantitative real-time PCR. *Biochem. Biophys. Res. Commun.* **313**, 856-862. doi:10.1016/j.bbrc.2003.11.177

Saunders, B. K. and Muller-Parker, G. (1997). The effects of temperature and light on two algal populations in the temperate sea anemone *Anthopleura elegantissima* (Brandt, 1835). *J. Exp. Mar. Biol. Ecol.* **211**, 213-224. doi:10.1016/S0022-0981(96)02723-2

Sebens, K. P. (1981). The allometry of feeding, energetics, and body size in three sea anemone species. *Biol. Bull.* **161**, 152-171. doi:10.2307/1541115

Secord, D. and Augustine, L. (2000). Biogeography and microhabitat variation in temperate algal-invertebrate symbioses: zooxanthellae and zoochlorellae in two Pacific intertidal sea anemones, *Anthopleura elegantissima* and *A. xanthogrammica*. *Invertebr. Biol.* **119**, 139-146. doi:10.1111/j.1744-7410.2000.tb00002.x

Seneca, F. O., Forêt, S., Ball, E. E., Smith-Keune, C., Miller, D. J. and van Oppen, M. J. H. (2010). Patterns of gene expression in a scleractinian coral undergoing natural bleaching. *Mar. Biotechnol.* **12**, 594-604. doi:10.1007/s10126-009-9247-5

Shick, M. J. (1991). Nutrition. In *A Functional Biology of Sea Anemones* (ed. P. Calow), pp. 36-118. Chapman and Hall.

Soubrier, J., Steel, M., Lee, M. S. Y., Der Sarkissian, C., Guindon, S., Ho, S. Y. W. and Cooper, A. (2012). The influence of rate heterogeneity among sites on the time dependence of molecular rates. *Mol. Biol. Evol.* **29**, 3345-3358. doi:10.1093/molbev/mss140

Tabita, F. R., Satagopan, S., Hanson, T. E., Kreel, N. E. and Scott, S. S. (2008). Distinct form I, II, III, and IV Rubisco proteins from the three kingdoms of life provide clues about Rubisco evolution and structure/function relationships. *J. Exp. Bot.* **59**, 1515-1524. doi:10.1093/jxb/erm361

Tansik, A. L., Fitt, W. K. and Hopkinson, B. M. (2015). External carbonic anhydrase in three Caribbean corals: quantification of activity and role in CO_2 uptake. *Coral Reefs* **34**, 703-713. doi:10.1007/s00338-015-1289-8

Tansik, A. L., Fitt, W. K. and Hopkinson, B. M. (2017). Inorganic carbon is scarce for symbionts in scleractinian corals. *Limnol. Oceanogr.* **62**, 2045-2055. doi:10.1002/lno.10550

Tashian, R. E. (1989). The carbonic anhydrases: widening perspectives on their evolution, expression and function. *BioEssays* **10**, 186-192. doi:10.1002/bies.950100603

Toguri, T., Muto, S., Mihara, S. and Miyachi, S. (1989). Synthesis and degradation of carbonic anhydrase in a synchronized culture of *Chlamydomonas reinhardtii*. *Plant Cell Physiol.* **30**, 533-539. doi:10.1093/oxfordjournals.pcp.a077772

Tresguerres, M., Barott, K. L., Barron, M. E., Deheyn, D. D., Kline, D. I. and Linsmayer, L. B. (2017). Cell biology of reef-building corals: ion transport, acid/base regulation, and energy metabolism. In *Acid-Base Balance and Nitrogen Excretion in Invertebrates: Mechanisms and Strategies in Various Invertebrate Groups with Considerations of Challenges Caused by Ocean Acidification* (ed. D. Weihrauch and M. O'Donnell), pp. 193-218. Cham: Springer International Publishing.

Verde, E. A. and McCloskey, L. R. (1996). Photosynthesis and respiration of two species of algal symbionts in the anemone *Anthopleura elegantissima* (Brandt) (Cnidaria; Anthozoa). *J. Exp. Mar. Biol. Ecol.* **195**, 187-202. doi:10.1016/0022-0981(95)00080-1

Verde, E. and McCloskey, L. (2002). A comparative analysis of the photobiology of zooxanthellae and zoochlorellae symbiotic with the temperate clonal anemone *Anthopleura elegantissima* (Brandt). II. Effect of light intensity. *Mar. Biol.* **141**, 225-239. doi:10.1007/s00227-002-0824-7

Verde, E. A. and McCloskey, L. R. (2007). A comparative analysis of the photobiology of zooxanthellae and zoochlorellae symbiotic with the temperate clonal anemone *Anthopleura elegantissima* (Brandt). III. Seasonal effects of natural light and temperature on photosynthesis and respiration. *Mar. Biol.* **152**, 775-792.

Weis, V. M. (1991). The induction of carbonic anhydrase in the symbiotic sea anemone *Aiptasia pulchella*. *Biol. Bull.* **180**, 496-504. doi:10.2307/1542351

Weis, V. M. (1993). Effect of dissolved inorganic carbon concentration on the photosynthesis of the symbiotic sea anemone Aiptasia pulchella Carlgren: role of carbonic anhydrase. *J. Exp. Mar. Biol. Ecol.* **174**, 209-225. doi:10.1016/0022-0981(93)90018-J

Weis, V. M. and Reynolds, W. S. (1999). Carbonic anhydrase expression and synthesis in the sea anemone *Anthopleura elegantissima* are enhanced by the presence of dinoflagellate symbionts. *Physiol. Biochem. Zool.* **72**, 307-316. doi:10.1086/316674

Weis, V. M., Smith, G. J. and Muscatine, L. (1989). A 'CO_2 supply' mechanism in zooxanthellate cnidarians: role of carbonic anhydrase. *Mar. Biol.* **100**, 195-202. doi:10.1007/BF00391958

Whelan, S. and Goldman, N. (2001). A general empirical model of protein evolution derived from multiple protein families using a maximum-likelihood approach. *Mol. Biol. Evol.* **18**, 691-699. doi:10.1093/oxfordjournals.molbev.a003851

Wickham, H. (2009). *ggplot2: Elegant Graphics for Data Analysis*, 1st edn. New York: Springer-Verlag.

Yang, Z. (1995). A space-time process model for the evolution of DNA sequences. *Genetics* **139**, 993-1005.

Zamer, W. E. (1986). Physiological energetics of the intertidal sea anemone *Anthopleura elegantissima* I. Prey capture, absorption efficiency and growth. *Mar. Biol.* **92**, 299-314. doi:10.1007/BF00392670

SUPPLEMENTARY INFORMATION

SUPPLEMENTARY FIGURES

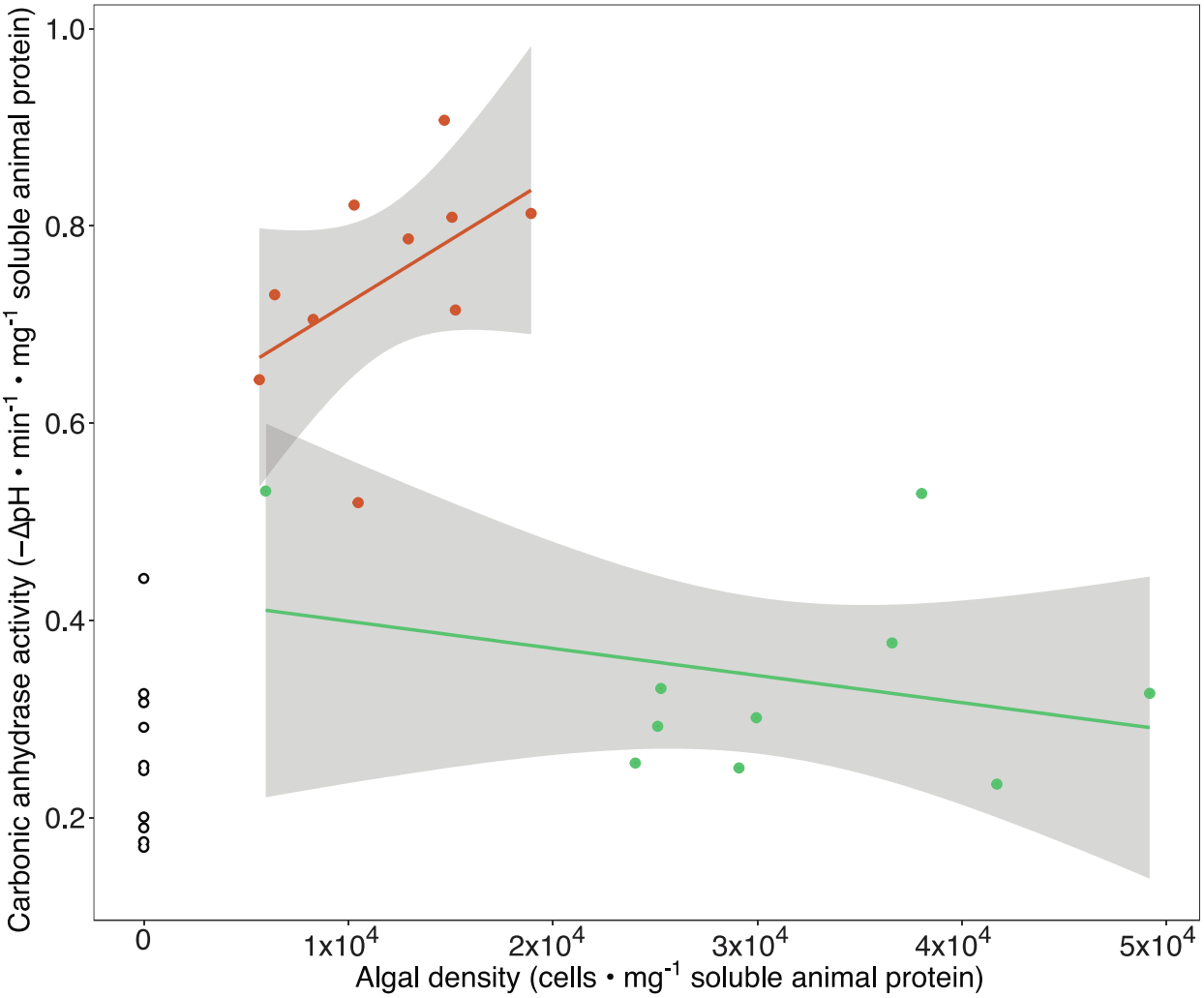

Figure S1. The relationship between algal density and CA activity from field-collected brown, green, and aposymbiotic *A. elegantissima*. Each point is the average of triplicate technical replicates. Colors: brown = brown, green = green, aposymbiotic = white. A linear model was fit for each set of symbiotic states in the data indicated by a brown or green line (brown: y = 0.000001278x + 0.5942, adjusted R^2 = 0.1626, F = 2.748, *p* = 0.136; green: y = -0.0000002752x + 0.4266, adjusted R^2 = -0.02078, F = 0.8168, *p* = 0.3925) with standard error of the model represented by the extent of the gray region around each line. There is no linear model for the aposymbiotic anemones since all individuals had no algae present.

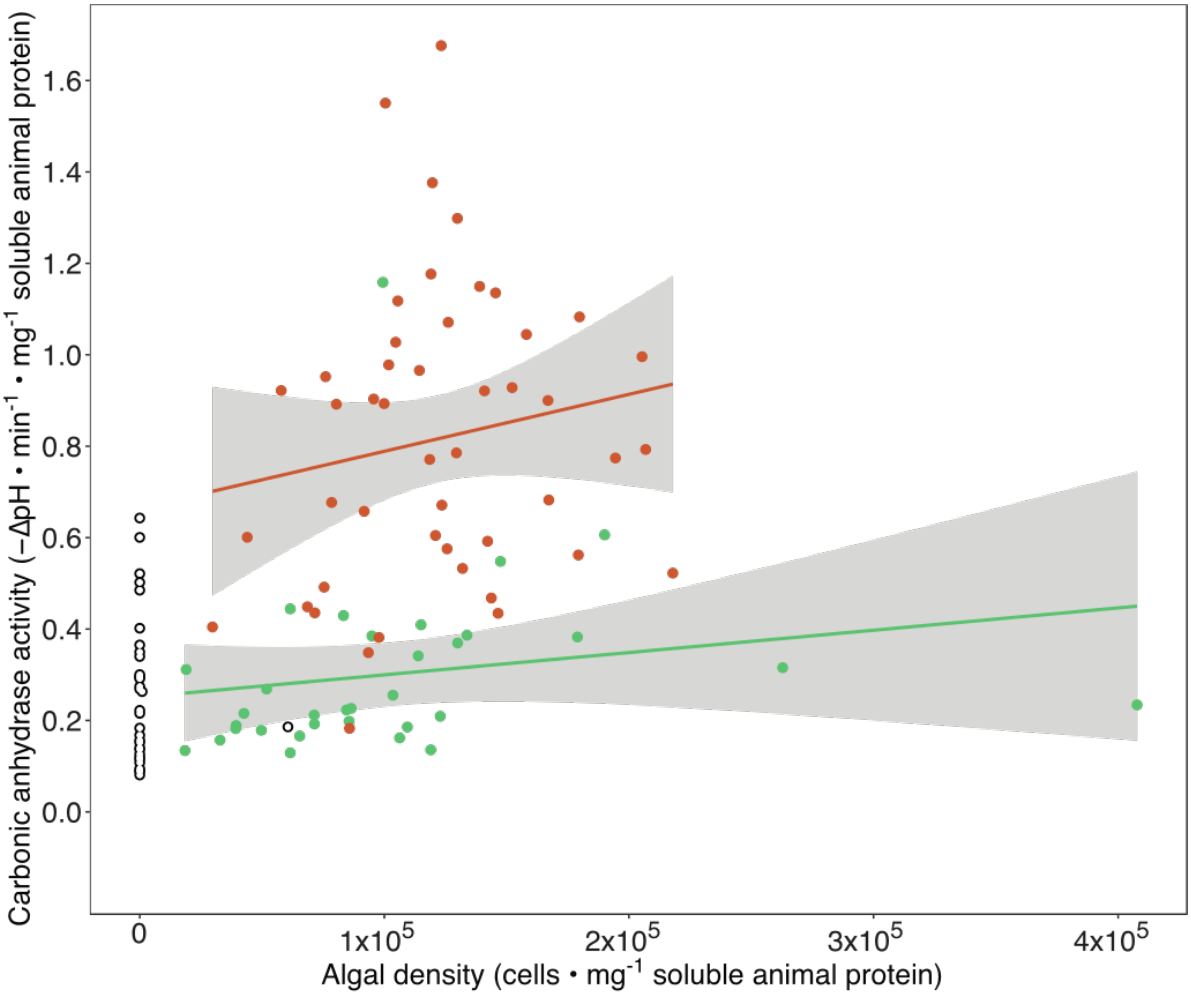

Figure S2. The relationship between algal density and CA activity from the light experiment. Each point is the average of triplicate CA and quadruplicate algal count technical replicates. Colors: brown = brown, green = green, aposymbiotic = white. A linear model was fit for brown and green states in the data indicated by a brown or green line, respectively. (brown: y = 0.000001247x + 0.6641, adjusted R^2 = 0.005193, F = 1.24, *p* = 0.2714; green: y = 0.0000004882x + 0.2509, adjusted R^2 = 0.003974, F = 1.128, *p* = 0.296474) with standard error of the model represented by the extent of the gray region around each line. There is no linear model for the aposymbiotic anemones because all individuals except one had no algae present.

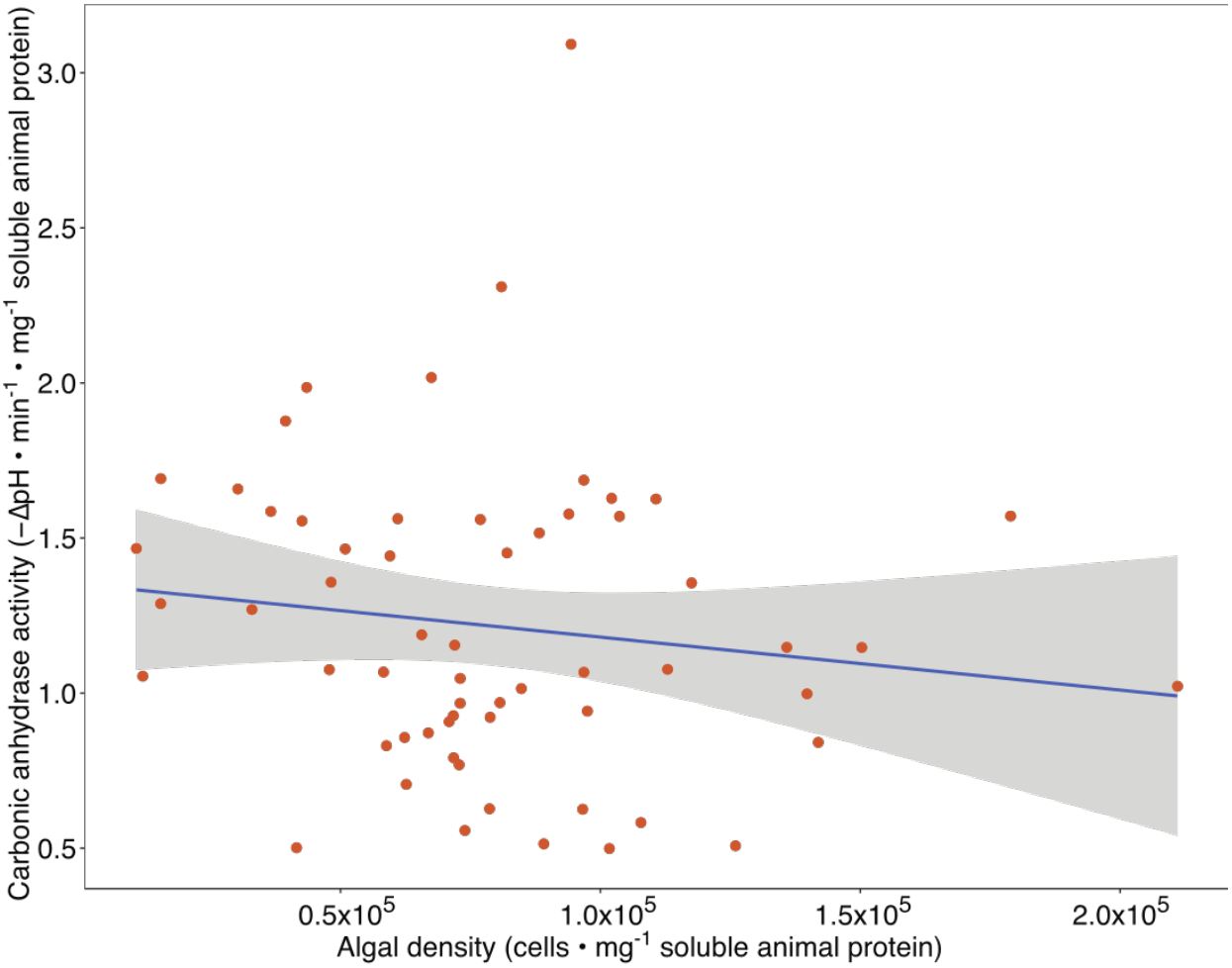

Figure S3. The relationship between algal density and CA activity from field-collected brown *A. elegantissima* of different sizes. Each point is the average of triplicate technical replicates. A linear model was fit to the data indicated by the blue line (y = -0.0000017x + 1.4, adjusted R^2 = 0.0014, F = 1.082, *p* = 0.303) with standard error of the model represented by the extent of the gray region around the line.

SUPPLEMENTARY TABLES

Table S1. Nucleotide and amino acid sequences for AeleCAs used in this study. Signal peptides, where present, are highlighted yellow and were excluded from phylogenetic analyses. Signal peptide with transmembrane regions, where present, are highlighted blue.

Gene	Nucleotide sequences	Protein sequences	Signal peptide?	Transmembrane domain?

AeleCA 1	Nucleotide: CTTCCGATCTACTTTGCATAAGCTAGCGTCGACTGCTGTTTGTTC CTGCAGAGCTGAGATCCACAACACTCACTTGTAAACCAAGATAT TGAGATGGCTGCACCAAAATGGGGTTATGGTCCTAATAACGGGC CTTCAAAATGGGCCAAGGATTTCCCTGCAGCCGCAGGGGCACG CCAATCACCGATCGACATCAAAACACATGATGCTCAACATGACA GTGCACTCAAAATAAAGCCCTTGAAAATCCAATACAGCCAGGGA AACGACTTCAATGTCACCAATAATGGCTACTCTTTGGTCATATCG CGCAAGACCAGTGAAGGGACTAACTTGAGTGGTGGGCCGTTG GAACATAACTACCGCTTTGAGCAGTTTCATTTCCACTGGGGAAA GACATCTGGAAGTGGCTCGGAGCATTTGCTGGATGGAAAAGCC TTTCCTGCAGAGCTTCATCTTGTTCACTGGAACACAGATCTCTTC AGCAGTTTTGGCGAAGCGGCGTCGAGTAAGAATGGCCTGGCTG TGCTTGGTGCCTTTGTGCAAATTGGTGGTGAAAGTGCTGGTCTG AAGACGATCACCGACATGATCCCCCAAGTCCAGAATATTGGCGA CAAACAAGACCTTAAGGTTCCCTTCAACTTATCGTCGTTGCTACC AAGTAACACTAATGACTACTGGACCTACAGTGGTTCCCTCACCAC CCCTCCCTGCTATGAAAGTGTCTCCTGGTTCGTTTTCAAGGAGC CAATCCACGCAACGGAGAATCAGATGCAGCAGTTCCGTTCACTC AAGGCCAACGATGGTGGATGTATAGTGGACAACTACAGACCAG TCATGGATGGTAGTGGACGCAACGTCAGGGCTTCTTTTGAGTGA AAAGTTTGGCATGAAAAATTAGAAACAAACTCTCGTAATTCTGA CCTTGAAAAGAACGAATGATCGAGGAACGTAGGAAGTATAGTT GTAATTTGTAGCCGAGATGAAGGCTTTTAGAATCTATAGAAATGT TGTAAACAAGAGAGACAGCAAATAAATATGAATTTGCCAAAAAA	Amino acid (frame 1, open reading frame 2 frame 1): MAAPKWGYGPNNGPSKWAKD FPAAAGARQSPIDIKTHDAQHDS ALKIKPLKIQYSQGNDFNVTNNG YSLVISRKTSEGTNLSGGPLEHNY RFEQFHFHWGKTSGSGSEHLLD GKAFPAELHLVHWNTDLFSSFGE AASSKNGLAVLGAFVQIGGESAG LKTITDMIPQVQNIGDKQDLKVP FNLSSLLPSNTNDYWTYSGSLTTP PCYESVSWFVFKEPIHATENQM QQFRSLKANDGGCIVDNYRPVM DGSGRNVRASFE*	Y	N

AeleCA 4	Nucleotide: TGTTGCTTACCAAGCTTGAAATATATTATATTAATGAATATGCAAAT AATGTCAGTACAGAAGAAAACATGCTGGAAAAACCAGCAGACA AATGCAAAGTTTGGGAAAATCCCATATAGTTGTTACCTTTCGCTG CTTGCATTCACATCACCCATACTGCATTTAGAGCTTGGTATAAGA CATGCAACAAGCAACAATACCTTCACCAACCTTTCTAAAAATAGC TGTTTATCGGACAACTCGATTACAACAAGACTGCTGCCGTCACA GCGGACAGAATGGTTGTCATGGTGGCGGTCACGAGATAAGATT CGCTGTCTGGTCCCTTATGATCAGCTGCAGTCTTGAAGCTTCTTT TGACGACACGAGAATTCAGAGGTTCAACGGGACGGAAGGTGT CGGTTAGAACACCTCTATCGTTGTCTTTTAGGCTTCGAAGCATGT CGAGCTGAGCTTGGGAGATTGTAGCGTAGTTCTTAAAGACGGT CCAAGTGACAACCTCGTTACAAGTTGGTGTTGTCAAACTACCCT TGTACCTGTAGAAGTCAGTGATGTTGGTTGGGAGTAAAGATGCC AGGTTGTTGGTCATAGACAAACCAGTTACTTTACTAGATGGGTG AGTCACATTGAGTGCGTACTTCAAAAAGGACGTCAGAGCTGTAT TTTCGGTTGTACCAACCTTGAAGATGACGCCTAAAACTGCAAGT CCATCTTCTTGTTTTACGGCTTCACCTATGTTTGAGTACTTTGTGT TGAAGTTCACAAAATGCAACTCAGCCGGGTACTTTGTCCCATCC ACGGTGTGTTCAGATCCCTTATTGTTTTCACTACCCCAGTGGAAA TGAAACTGGAGAGTGGTGAAAGTACCTGGTAACCCTCCTTTGG ACACGAGGAATGTGTTGGGTGTAAAGAACACTGTATAGGAATG ACCATTGTTAGATACATTAAATTTTGCCCCAGTGGGAACAGTGTT GAATTTGGTCAGGGTGAGTTTTTCCAAACTTGCGTCGTATTCAG TTTTAGAGGCTTCAATGTCGATGGGCGACTGGCTTGAACCGTTA CAAAAGCTTGGAAACGTTTTAGCCCAGCCAAGAGGACCATACT TGGTATCTGTGACATTGTAATTGAAACTATTAGAAGCCCCAAGCA TAGGTTGAACCAATGCCAAAATAAGTACACAACTTAGTGAAAGA TTTATTGCCATGTTTCGTGGAGAGAAAAAAGTTTTCATTAAGCA AAAATTACCTTTCGGTATCGTATCTGGTTATTCCTGTCTTTTTCTG TTTTCCTTTTGGCTTCATATAGCTAGTGATTATAGTGTTTCAGTTG TCCATAACTGTTGATTAGACTATTATACTATTCGTTGCCTGTGGAG	Amino acid (frame 3 reverse, open reading frame 13 frame 3): MKTFFSPRNMAINLSLSCVLILAL VQPMLGASNSFNYNVTDTKYGP LGWAKTFPSFCNGSSQSPIDIEAS KTEYDASLEKLTLTKFNTVPTGAK FNVSNNGHSYTVFFTPNTFLVSK GGLPGTFTTLQFHFHWGSENNK GSEHTVDGTKYPAELHFVNFNTK YSNIGEAVKQEDGLAVLGVIFKV GTTENTALTSFLKYALNVTHPSSK VTGLSMTNNLASLLPTNITDFYR YKGSLTTPTCNEVVTWTVFKNYA TISQAQLDMLRSLKDNDRGVLTD TFRPVEPLNSRVVKRSFKTAADH KGPDSESYLVTATMTTILSAVTAA VLL*	N	Y

AeleCA 6	Nucleotide: ATATTCCCAAATTCAAGAACATACCAAAATGATCCTCGTGTTTTTC ACGCTTCTTCAAACTTTTCGTGTTTTGATTGATGAGAAACGAAC AGATAAGTAAAACTTTTCACTAATATTTTCTCTACTTTTAATCAGT AGTCATGATTTTATTCTGACACTTTTTCATTCGTGCAGTGTTACTC TTCGCCCGTTGAGGGGTAGGGTAGGTCTGTAGTTGTTGCACATT TTGCCGTGATGGTAGCCATGTGTAGCCTGGAGGGCTCTGAAATT ATTCAGAATTTCTTGGTCAGCAGTGATAGGAGTTCTGAGCACTAT CCATCGAACAGACTCGTAACATCCAGGGGTGGTCAGGGATCCCT TGTATGTGTAGTATGATCTACCACCAGACGATAGACCACCAACCA AGCTATCGAGTCTGACGGCAACTCCAGCTTTCTGAGATCCTTCT GTTATTATTGCATTCAAATTCAGTGAAAACGTCTTAAGTTCTGGT GCTCCAGAAGATCCCTTCTTCAGGAAAGCACCAATCACTGTCAA GCCGTCTGATTTGGTGGCAGCGGTGGAGATGTCGCCATATTTGG CGTTATAGAACACCAAGTGAAGCTCTCCTGGGTAAGATCTGCCA TTGATTGTGTGCTCCGAACCAACATTATCAGTACATCCGAAATGG AAGTGAAACTGAGCAAGGATATATTTCTGACCATTAACTGGATTA TATACACTTGCACTACCTTTCTCAACGTTGAAAGTTGGTGAATGC CCATTGTTGACCAGAGTTCCTTTGACCGTCCCCCAATAATACTGA AACCTTACACGCAGTGGACGGAGGTCGATATCATCACCATCTTT GACTTTAGCACGGACGATGTTTACTGGAGATTGGGAACGAGCA TTGCAATCCTTGGATACGTGACCCCAGTCTGATGGTCCATACACT TGACCATAAGTCTTGCCATAACCCCAAGAACCGGCTGAGGATGC CAGGCCAAAGAATCCAGCACTCAACACTATGATCTGCATCAACA TCATCGTTTTCTTTAATATTCAATGAGAAACGTCGTAAATATCGAA GTAAATAAGGACAAGGTGTTTGAGCGTGATGGCGATAAAGGTT TGTGTTGAGTGCTGGATTCTTTGGCCTGGCATCCTCAGCCGGTT CTTGGGGTTATGGCAAGACTTATGGTCAAGTGTATGGACCATCA GACTGGGGTCACGTATCCAAGGATTGCAATGCTCGTTCCCAATC TCCAGTAAACATCGTCCGTGCTAAAGTCAAAGATGGTGATGATAT CGACCTCCGTCCACTGCGTGTAAGGTTTCAGTATTATTGGGGGA CGGTCAAAGGAACTCTGGTCAACAATGGGCATTCACCAACTTTC	Amino acid (frame 3 reverse, open reading frame 13 frame 3): MMLMQIIVLSAGFFGLASSAGS WGYGKTYGQVYGPSDWGHVSK DCNARSQSPVNIVRAKVKDGDD IDLRPLRVRFQYYWGTVKGTLVN NGHSPTFNVEKGSASVYNPVNG QKYILAQFHFHFGCTDNVGSEHT INGRSYPGELHLVFYNAKYGDIST AATKSDGLTVIGAFLKKGSSGAPE LKTFSLNLNAIITEGSQKAGVAVR LDSLVGGLSSGGRSYYTYKGSLTT PGCYESVRWIVLRTPITADQEILN NFRALQATHGYHHGKMCNNYR PTLPLNGRRVTLHE*	Y	N

AeleCA 9	Nucleotide: AGGAACTAAGGTAGAGGTAACTGCATCATCTTTCATTGAATTGTT CAACAGAAGTCTCAAATACAAGGATGGCAAACACATTTCTAATT TTCCTAACAGCAGCAATTTTTCAAGTCTCGCTGAGTGTCGATTAC AATTATGAACTTTCAGACACCACCTATGGTCCTCTTGGTTGGCCC AAAACATACAATCCATCCTGTGACGGCTCCAGACAATCACCAATC AACATTAAGCCTTCAGATGCTAGCTATGATGGCTCGTTGGGAGA GCTGAGTTTCAAGAACTATAACCTTCCTGTCGATTCCGTGCTCAA GCTTGGAAACAATGGCAAATCCTACAGAGTGTTCTTCGAACCCA ATACGTACACGATATCCGGAGGAGGGCTGCCTGGTACTTTCTAC ACACATAACTTTCATTTCCACTGGGGTGCAGCTAACACCAAGGG ATCTGAGCATACTATTGATGGAAAGAAGTTCCCACTTGAGCTCCA TTTTGTTAATGTCAACACAAAGTACGCAACTGTTGCAGAAGCTT TACAACAGAAAGATGGGATTGCAGCAGTGGGCATCCTATACGA GGTTGGCGACGAAGATCTAGCGCTTGAACCTTTCTTAAAATACA CAGCTAATGTGACTTACAAAAGGGACATCTCGAATGTGACCGTG ATGGCTCAAGCCCTACAGACCCTTCTACCCCAAAACACCACTGA CTTCTATAGATATAACGGGTCTCTGACAACACCCAACTGCCAAGA AGTTGTCACATGGACTGTGTTTAAGAACTATCGAACAATCTCCCA AGCACAGCTGGATATGCTTCGAAGTCTTAGAGCCACAAACAACG TAACCATGCTGGTAGACACATTCCGCCCTGTTCTACCTCTAGGTT CTCGTGTTGTTAAGAAAACCTTTCACACCAGCCATGGAGAAGCG TATCACGTGACTAACACCATGACGATTATTGCGTTCGTCGTCATG GCAATGGTTATGTCCAAGTAGTTTCACATTTTTTTGATGTAGTTT GTTTGTTAGCTTTTCAGTGCAAGGCTTTATCATTAAACTGATAAG CGCTTCAAAAAGCAATTTTCTACTTTCACATTCCCCAATACGTTAC AGTTTTTGGGTAACCAGGTTAAAAACAGCCGCAATTATTATGCT GAAGACTGATCAGAAGATGTTAGAAATGCATCTCATAATATAAGA AACAACCAGAAACAAAAAGAAAGAAATTTGCATATTTGGAAAA CTTTTGATATCTCTGCAACAAATTGATATATCAACAAACTGTAAAC GCTATCTGACTTTTTAAAACAACCCTTCCAAGTTACAGTTAAAAC TTGAAGCAAAATATTTCGTTTTAATTCATATAAATTTTGATGAAAT	Amino acid (frame 3, open reading frame 1 frame 3): LHHLSLNCSTEVSNTRMANTFLIF LTAAIFQVSLSVDYNYELSDTTYG PLGWPKTYNPSCDGSRQSPINIK PSDASYDGSLGELSFKNYNLPVD SVLKLGNNGKSYRVFFEPNTYTIS GGGLPGTFYTHNFHFHWGAAN TKGSEHTIDGKKFPLELHFVNVN TKYATVAEALQQKDGIAAVGILYE VGDEDLALEPFLKYTANVTYKRDI SNVTVMAQALQTLLPQNTTDFY RYNGSLTTPNCQEVVTWTVFKN YRTISQAQLDMLRSLRATNNVT MLVDTFRPVLPLGSRVVKKTFHT SHGEAYHVTNTMTIIAFVVMAM VMSK*	N	N

Table S2. Primers for qPCR experiments.

Gene name	Transcriptome identifier	qPCR primers
AeleCA6	comp404_c4_seq3	Forward: 5’-ACC AGA GTT CCT TTG ACC GTC-3’
		Reverse: 5’-CTG GGG TCA CGT ATC CAA GG-3’
AeleCA9	Comp2502_c1_seq3	Forward: 5’-TCG ATT CCG TGC TCA AGC TT-3’
		Reverse: 5’-ATC CCT TGG TGT TAG CTG CA-3’
AeleCA4	comp34611_c0_seq1	Forward: 5’-TAC AAC AAG ACT GCT GCC GT-3’
		Reverse: 5’-CTT CCG TCC CGT TGA ACC TC-3’
AeleCA1	comp7398_c0_seq2	Forward: 5’-CGC CAA TCA CCG ATC GAC AT-3’
		Reverse: 5’-TTC ACT GGT CTT GCG CGA TA-3’
G3PD		Forward: 5’-AGA GGC CTT CTT CAC AGC AC-3’
		Reverse: 5’-GTT GGC AAG GTC ATC CCA GA-3’
NADH		Forward: 5’-ATG GGA TTT GCT GGT CCA CT-3’
		Reverse: 5’-TGG GTA GAC AGG TTC ATC GT-3’